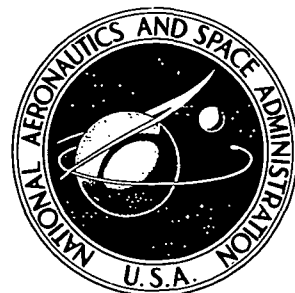


N72-31185

NASA TECHNICAL NOTE

NASA TN D-6959



CASE FILE
COPY

NASA TN D-6959

NUMERICAL METHOD AND FORTRAN PROGRAM
FOR THE SOLUTION OF AN AXISYMMETRIC
ELECTROSTATIC COLLECTOR DESIGN PROBLEM

by Oliver W. Reese

Lewis Research Center
Cleveland, Ohio 44135

NATIONAL AERONAUTICS AND SPACE ADMINISTRATION • WASHINGTON, D. C. • SEPTEMBER 1972

1. Report No. NASA TN D-6959	2. Government Accession No.	3. Recipient's Catalog No.	
4. Title and Subtitle NUMERICAL METHOD AND FORTRAN PROGRAM FOR THE SOLUTION OF AN AXISYMMETRIC ELECTROSTATIC COLLECTOR DESIGN PROBLEM		5. Report Date September 1972	
7. Author(s) Oliver W. Reese		6. Performing Organization Code	
9. Performing Organization Name and Address Lewis Research Center National Aeronautics and Space Administration Cleveland, Ohio 44135		8. Performing Organization Report No. E-6872	
12. Sponsoring Agency Name and Address National Aeronautics and Space Administration Washington, D.C. 20546		10. Work Unit No. 111-05	
15. Supplementary Notes		11. Contract or Grant No.	
		13. Type of Report and Period Covered Technical Note	
		14. Sponsoring Agency Code	
16. Abstract <p>This report describes the numerical calculation of the steady-state flow of electrons in an axisymmetric, spherical, electrostatic collector for a range of boundary conditions. The trajectory equations of motion are solved alternately with Poisson's equation for the potential field until convergence is achieved. A direct (noniterative) numerical technique is used to obtain the solution to Poisson's equation. Space charge effects are included for initial current densities as large as 100 A/cm^2. Ways of dealing successfully with the difficulties associated with these high densities are discussed. The report includes a description of the mathematical model, a discussion of numerical techniques, results from two typical runs, and the FORTRAN computer program.</p>			
17. Key Words (Suggested by Author(s)) FORTRAN Design Electrostatic Poisson Collector		18. Distribution Statement Unclassified - unlimited	
19. Security Classif. (of this report) Unclassified	20. Security Classif. (of this page) Unclassified	21. No. of Pages 67	22. Price* \$3.00

* For sale by the National Technical Information Service, Springfield, Virginia 22151

CONTENTS

	Page
SUMMARY	1
INTRODUCTION	1
STATEMENT OF THE PROBLEM	4
METHOD OF SOLUTION	5
Auxiliary Equations	8
The Equation of Motion	9
Poisson's Equation	10
Calculation of Space Charge	10
Use of Irregular Mesh Spacing	13
Convergence Acceleration	14
FORTRAN PROGRAM	14
General Description	14
Using the Program	16
CONCLUDING REMARKS	17
APPENDIXES	
A - SAMPLE PROBLEMS	19
B - FORTRAN PROGRAM	28
C - FORTRAN SYMBOLS	50
D - FLOW CHARTS	54
E - MAGNETIC FIELD CALCULATIONS	57
F - DERIVATION OF EQUATIONS OF MOTION	61
G - MATHEMATICAL SYMBOLS	63
REFERENCES	65

NUMERICAL METHOD AND FORTRAN PROGRAM FOR THE SOLUTION OF AN AXISYMMETRIC ELECTROSTATIC COLLECTOR DESIGN PROBLEM

by Oliver W. Reese

Lewis Research Center

SUMMARY

This report describes the determination of the steady-state flow of electrons in an axisymmetric spherical collector under a variety of boundary conditions. The electron trajectory equations of motion are solved alternately with Poisson's equation for the potential field until convergence is achieved.

The bounding surfaces are a sphere below, a spherical cone above, and, optionally, a thin axial spike suspended from the apex of the cone. Negative decelerating potentials are prescribed on the cone-spike surface and on segmented zones of the spherical surface. Polar angles of the cone may vary from 0° to 160° .

The principal value of this report is that it pushes design research into the high-current-density range, where space charge effects are strong. Initial attempts met with convergence difficulties for current densities above 50 A/cm^2 .

This report describes the method used to surmount these difficulties and handle values as high as 100 A/cm^2 . This was achieved in two ways: first, by using variable mesh spacing to ensure accuracy in regions where the solution was changing rapidly; and second, by using a fast, accurate subprogram for obtaining the potential field. This subprogram uses a direct, noniterative numerical solution to Poisson's equation, the details of which are given in NASA TN D-6438.

The present report includes a description of the mathematical model, a discussion of numerical techniques, results from two typical runs, and the FORTRAN computer programs.

INTRODUCTION

Satellite communication systems have been proposed in which the satellite can receive, amplify, and rebroadcast microwave signals. The high efficiency of the micro-

wave amplifiers to be used is of prime importance to the lifetime and reliability of such a system.

Microwave amplifiers, as a class, convert the energy of bunched electron beams into radiofrequency (rf) energy. Since this process is only partially efficient, the remaining beam energy is dissipated as heat in the electron collector. However, collectors can be designed and maintained at proper potentials to slow the electrons. The electron energy is then spent doing work against the collector potential and is recoverable as useful electrical power.

Reference 1 discusses how the results of the program described in this report are used in collector design. Reference 2 describes a computer program which solves Poisson's equation for a given space charge and which is required as a subroutine in the iterative solution of the current problem.

It is important to realize that there are two characteristics of electron beam trajectory patterns that facilitate efficient collector design:

- (1) Good, uniform, vertical and horizontal spreading (i.e., a sufficient rise away from the entry hole, and a pushing away from the collector axis)
- (2) Good, uniform separation permitting insertion of electrodes to collect electrons near the peak of their trajectories, where their energy is close to minimum

Both these characteristics imply no backstreaming, crossing, or impingement of beams on the underside of the electrodes.

The original computer program dealt with negative decelerating potentials prescribed only on segmented zones of the sphere. But this approach was ineffective because of the great distance between these surface potentials and the incoming stream of electrons.

A second stage of the design was to prescribe a decelerating potential on a cone of varying polar angle. This slowed down the incoming stream considerably, and in most cases the beam spread was sufficient.

In other instances where even more beam spread was desirable, a third and final design modification was made. Here a negative potential was prescribed on a thin spike suspended from the cone. This had the effect of spreading the flow even more as it entered, and allowing the other decelerating potentials to come into play more effectively.

The final FORTRAN program reported herein allows for the presence or absence of an axial spike of varying length, as well as for the choice of decelerating surface potentials on zonal segments of the sphere and on the cone-spike surface. The cone angle varies from 0° to 160° . Initial conditions also include variable velocity and injection positions of entering electron groups.

It was assumed that, prior to entry into the collector, the electron beam had been sorted into graded velocity groups, with the outermost being the slowest. This is physically more realistic than assuming a constant velocity only. The beam was then

injected through a small entry hole in the collector where the negative polar axis pierces the spherical surface. The potential distribution on the surface of the sphere was assumed to be a function of the polar angle only. This report describes the numerical solution to a problem used in the design of such a collector under varying conditions of surface potential, current density, and collector geometry.

A typical configuration is shown in figure 1. Notice that the electron groups reach minimum velocity at their peaks and start falling back. If electrodes of the proper potential are inserted to collect the electrons at these minimum velocity points, the efficiency of the collector will then be maximized.

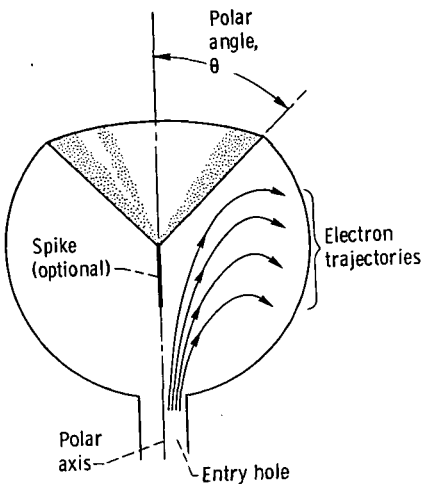


Figure 1. - Typical collector geometry (spherical cone).

The numerical technique and computer program described in reference 2 were used to determine the potential field inside the collector as required. The results were then used as part of the design criteria of the collector as described in reference 1.

In situations where current density is low, less than 10 A/cm^2 , space charge effects were found to be negligible. But with higher current densities and associated higher space charge, certain problems arise near the entry hole that require special techniques to ensure numerical stability. This report describes these techniques. Current densities as high as 100 A/cm^2 were dealt with successfully. Initially, calculations were successful only with current densities half as large, before numerical difficulties precluded further computation.

A complete description of the mathematical model is given, along with a discussion of the assumptions made. The technique used in determining the space charge distribution is then described. Appendixes A to G contain the results of two typical computer

runs, a complete listing of the FORTRAN computer program, flow charts, magnetic field calculations, the derivation of the equations of motion, and the mathematical symbols.

STATEMENT OF THE PROBLEM

The problem is to determine the steady-state potential field and the associated steady-state electron beam trajectory patterns within a spherical collector (1) for any specified collector geometry (cone angle; collector radius; entry hole radius; and length of axial spike, if any), (2) for negative potential distribution on the surfaces of the collector, and (3) for magnetic field distribution and electron beam initial entry conditions (current, current density, perveance, injection angles, positioning, and velocity).

This involves the determination at every mesh point in the sphere of the potential V that satisfies Poisson's equation

$$\nabla^2 V = \bar{f}(V) \quad (1a)$$

where

$$\nabla^2 V = \frac{\partial^2 V}{\partial \bar{\rho}^2} + \frac{2}{\bar{\rho}} \frac{\partial V}{\partial \bar{\rho}} + \frac{1}{\bar{\rho}^2} \frac{\partial^2 V}{\partial \theta^2} + \frac{\cot \theta}{\bar{\rho}^2} \frac{\partial V}{\partial \theta} + \frac{1}{\bar{\rho}^2 \sin^2 \theta} \frac{\partial^2 V}{\partial \varphi^2} \quad (1b)$$

The bars refer to dimensioned values. All mathematical symbols are defined in appendix G. For convenience, these expressions and all others following are normalized by the substitution

$$\rho = \frac{\bar{\rho}}{R} \quad (1c)$$

We may now write

$$f(V) = \frac{\rho_e(V)}{\epsilon_0} \quad (1d)$$

The right-hand term in equation (1d) is related to space charge resulting from the beam trajectories. These trajectories are obtained from the solution to the differential equation of motion (eq. (3)). Note that the determination of V is an iterative process,

in that the right-hand side (or source term), which depends on the space charge, changes when the internal potential V changes.

The source term consists of the dielectric constant ϵ_0 and $\rho_e(V)$ where

$$\rho_e(V) = \frac{|\vec{J}|}{|\vec{u}|} \quad (2)$$

The velocity term u is easily calculated since it is simply a function of certain initial conditions and the potentials V and V_m .

The current density term J is somewhat more complicated. In general, it is calculated from the current flow through annuli formed by adjacent trajectories of the various electron energy groups. This flow is shown later in figure 4. These trajectories are calculated from the differential equation of motion

$$\begin{aligned} \frac{\partial^2 \rho}{\partial \theta^2} = \rho'' = \rho + \frac{\rho \sin^2 \theta \dot{\varphi}^2}{\dot{\theta}^2} + \frac{\eta}{\dot{\theta}^2 R} \left(\frac{1}{R} \frac{\partial V}{\partial \rho} - \sin \theta \dot{\varphi} \frac{\partial V_m}{\partial \theta} \right) - \frac{\rho' \sin \theta \cos \theta \dot{\varphi}^2}{\dot{\theta}^2} \\ + \frac{2\rho'^2}{\rho} - \frac{\rho' \eta}{\rho^2 \dot{\theta}^2 R^2} \left(\frac{\partial V}{\partial \theta} + \rho^2 R \sin \theta \dot{\varphi} \frac{\partial V_m}{\partial \rho} \right) \end{aligned} \quad (3)$$

where

ρ normalized radius vector

θ polar angle

φ azimuthal angle

R radius of sphere

V_m magnetic field

Details of this iterative process are described in the next section.

METHOD OF SOLUTION

First, the steady-state flow of electrons with a given velocity distribution was determined within the collector. This was accomplished by taking the following four steps:

(1) With the given collector geometry and a specified set of initial conditions, a first approximation to the potential field inside the collector was found by assuming zero space charge and solving Laplace's equation

$$\nabla^2 V = 0 \quad (4)$$

or

$$\frac{\partial^2 V}{\partial \rho^2} + \frac{2}{\rho} \frac{\partial V}{\partial \rho} + \frac{1}{\rho^2} \frac{\partial^2 V}{\partial \theta^2} + \frac{\cot \theta}{\rho^2} \frac{\partial V}{\partial \theta} = 0 \quad (5)$$

(2) An arbitrary number of equally spaced electron trajectories were then calculated from the equation of motion (eq. (3)). This equation is derived in appendix F. In general, nine electron groups were solved for in this problem.

(3) From these trajectory patterns, the space charge was then calculated at each mesh point, and the results were used as source terms in Poisson's equation which was solved next,

$$\nabla^2 V = \frac{\rho e}{\epsilon_0} \quad (6)$$

Details of how the space charge was calculated are given in a later section.

(4) Equation (3) was solved again to obtain new trajectories based on the new potential field obtained from equation (6). This iterative process was then continued until convergence was achieved. The entire process is shown in flow chart form in figure 2.

Prior to solving the problem, the following four sets of normalized initial conditions must be specified. (The quantities listed in the first three sets are shown in figure 3 for the case of three electron classes.)

- (1) Collector geometry: radius of collector R , initial polar angle θ_0 , and radius of entry hole a
- (2) Collector boundary values of electric potential: on a spherical surface (V_1, V_2, \dots, V_f) (In general, the potential on the spherical surface decreases linearly to zero ($V_f = 0$) as the polar angle increases from θ_0 to some prescribed θ_f .); on a conical surface if $\theta_0 \neq 0(V_1)$; and along the negative polar axial spike if $\theta_0 \neq 0(V_1)$ (optional)
- (3) Electron beam entry conditions: type of flow (Brillouin or confined; confined flow means there is no initial rotational velocity of the beam, or $\dot{\phi} = 0$), values of beam energy classes v_i , entry positions of electron classes in hole at injection δ_i (δ_i is the supplement of the polar angle θ), and entry angles α_i . In general, $i = 1, 2, \dots, 9$.

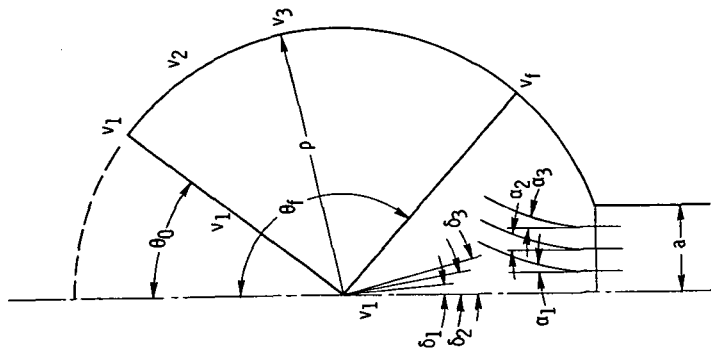


Figure 3. - $p\text{-}\theta$ plane of a typical axisymmetric collector, showing various initial conditions.

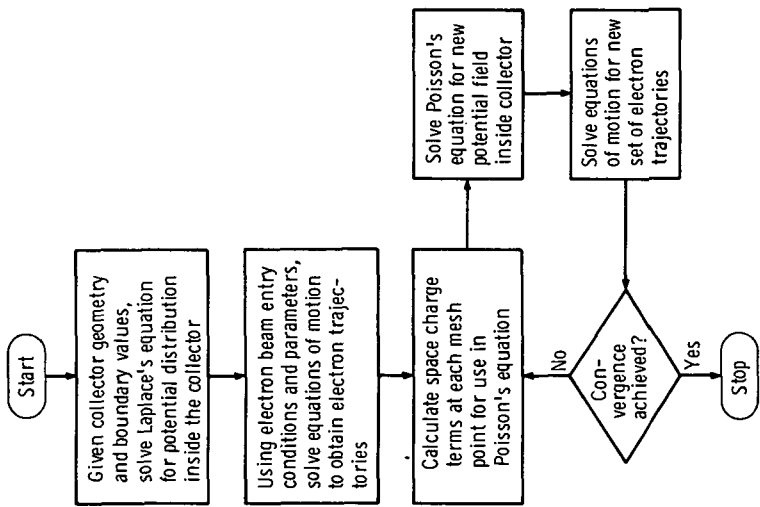


Figure 2. - Flow of operations in solution of complete problem.

(4) Electron beam parameters: magnetic flux density B_0 , magnetic field potential V_m , electric potential V_0 , current I_0 , and current density J_0

Auxiliary Equations

We now discuss the auxiliary equations which are required in the solution of equation (3).

The first two are the magnetic field terms expressed in cylindrical coordinates.

$$\frac{\partial V_m}{\partial \rho} = R \left(\frac{\partial V_m}{\partial r} \sin \theta + \frac{\partial V_m}{\partial z} \cos \theta \right) \quad (7a)$$

$$\frac{\partial V_m}{\partial \theta} = \rho R \left(\frac{\partial V_m}{\partial r} \cos \theta - \frac{\partial V_m}{\partial z} \sin \theta \right) \quad (7b)$$

or letting $B_r = \partial V_m / \partial r$ and $B_z = \partial V_m / \partial z$, then

$$\frac{\partial V_m}{\partial \rho} = R(B_r \sin \theta + B_z \cos \theta) \quad (8a)$$

$$\frac{\partial V_m}{\partial \theta} = \rho R(B_r \cos \theta - B_z \sin \theta) \quad (8b)$$

Prior to entering the collector, the electron beam passes through a magnetic field which is used to confine the beam. Part of this field leaks into the collector through the entry hole and influences the flow of the electrons. It must be considered in the equations of motion.

Also used are the velocity terms, $\dot{\theta}^2$ and $\dot{\phi}$, and the magnetic flux ψ . These are expressed as

$$\dot{\theta}^2 = \frac{1}{1 + (\rho'/\rho)^2} \left[\frac{2\eta_e V_0 (v_i + V)}{\rho^2 R^2} - \dot{\phi}^2 \sin^2 \theta \right] \quad (9)$$

$$\dot{\phi} = \frac{\eta_e (\psi - \psi_0)}{2\pi\rho^2 R^2 \sin^2 \theta} \quad (10)$$

$$\psi = 2\pi \int_0^r B_z r dr \quad (11)$$

which are equations (B16), (B8), and (B9) of reference 1, respectively.

Finally, the components B_r and B_z of the magnetic field V_m (eqs. (D9) and (D10) of ref. 1) are expressed as

$$B_r(r, z) = \sum_{n=0}^{\infty} \frac{(-1)^n}{n!(n+1)!} \times \frac{\partial^{2n+1} B(0, z)}{\partial z^{2n+1}} \times \left(\frac{r}{2}\right)^{2n+1} \quad (12)$$

and

$$B_z(r, z) = \sum_{n=1}^{\infty} \frac{(-1)^{n+1}}{[(n-1)!]^2} \times \frac{\partial^{2n-2} B(0, z)}{\partial z^{2n-2}} \times \left(\frac{r}{2}\right)^{2n-2} \quad (13)$$

where

$$B(0, z) = B_0 \left[1 - \frac{1}{\pi} \tan^{-1} \left(\frac{a}{z} \right) - \frac{1}{\pi} \frac{z/a}{1 + (z^2/a^2)} \right] \quad (14)$$

The approximations of $B_r(r, z)$ and $B_z(r, z)$ that were used are given in appendix E.

The Equation of Motion

The second-order differential equation of motion (eq. (3)) was transformed into two first-order equations and solved by using a fourth-order Runge-Kutta method. As is typical in integration techniques of this type, the choice of step size is based largely on experience. In this problem, the most critical region is near the entry hole. For a large collector radius ($R = 16$ cm) and a small entry hole ($a = 0.05$ cm), an initial step size $\Delta\theta$ of 0.01° was required. For a small collector radius ($R = 8$ cm) and a large entry hole ($a = 0.10$ cm), an initial $\Delta\theta$ of 0.05° was sufficient. As the trajectory moved away from this critical region, the $\Delta\theta$ step was increased to minimize computer execution time.

Initially, the solution was obtained in the ρ - θ spherical plane. Then when any par-

ticular trajectory started to arc over ($\rho' \cong 0$), a change was made to the r-z cylindrical coordinate system to avoid any possible discontinuities in the integration process.

Poisson's Equation

For any space charge field, the set of right-hand sides for Poisson's equation written at all interior grid points may be computed, and the subroutine of reference 2 may be applied to solve Poisson's equation for the internal potential field. The method of calculating the space charge field from the trajectory field is now presented.

Calculation of Space Charge

The source term, or space charge term, in equation (6) is

$$\frac{\rho_e}{\epsilon_0} \quad (15)$$

where

ϵ_0 dielectric constant, 8.86×10^{-14} F/cm (farads per centimeter)

ρ_e volume charge density, C/cm³ (coulombs per cubic centimeter)

Furthermore,

$$\rho_e = \frac{J}{u} \quad (16)$$

where

J current density, A/cm² (amperes per square centimeter)

u velocity, cm/sec

Figure 4 shows where a typical ρ_e is computed; namely, at a point midway between two trajectories. To ensure accuracy, space charge is calculated at selected points along center lines midway between adjacent trajectories where the ρ -mesh lines are crossed.

Since u is known at various points along a trajectory, one may interpolate to compute u at any point, say at a position midway between two trajectories. Therefore, the

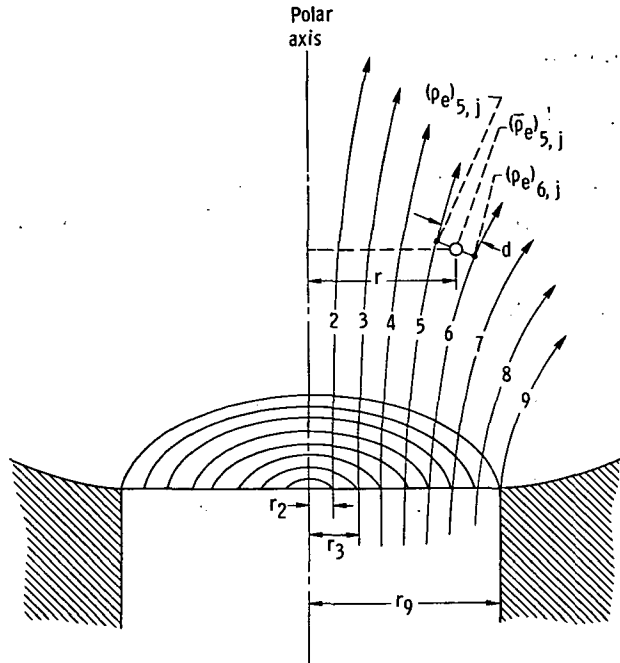


Figure 4. - Cross-sectional view of entry hole in spherical collector, showing typical injection pattern of electron energy groups 2 to 9 at radii r_2 , r_3 , ..., r_9 . First subscript refers to electron trajectory number; second subscript j refers to p-mesh line crossed by trajectory.

space charge at each mesh point may be determined once J is known. We now show how this is accomplished.

In general,

$$J = \frac{I}{A} \quad (17a)$$

where

I current, A

A any particular element of area through which current flows

Referring again to equation (6), we may now write

$$J_i = \frac{I_{0,i}}{A_i} \quad (17b)$$

where

I_0 initial current at injection

i i^{th} electron energy group

Referring again to figure 4, it is seen that the equally spaced electron energy groups form eight annuli at the entrance hole. The areas dA of these annuli may be expressed

$$\left. \begin{aligned} dA_1 &= \pi r_2^2 \\ dA_2 &= \pi r_3^2 - dA_1 = \pi(2r_2)^2 - dA_1 = 3 dA_1 \\ dA_3 &= \pi r_4^2 - \pi r_3^2 = \pi(3r_2)^2 - \pi(2r_2)^2 = 5 dA_1 \\ &\cdot \\ &\cdot \\ dA_8 &= \pi r_9^2 - \pi r_8^2 = \pi(8r_2)^2 - \pi(7r_2)^2 = 15 dA_1 \end{aligned} \right\} \quad (18)$$

Since $I = JA$, the current at injection through each annulus may be expressed

$$\left. \begin{aligned} I_{0,1} &= J_0 dA_1 \\ I_{0,2} &= J_0 dA_2 = 3J_0 dA_1 \\ I_{0,3} &= J_0 dA_3 = 5J_0 dA_1 \\ &\cdot \\ &\cdot \\ I_{0,8} &= J_0 dA_8 = 15J_0 dA_1 \\ &\cdot \\ &\cdot \\ I_{0,i} &= (2i - 1)J_0 dA_1 \end{aligned} \right\} \quad (19)$$

In the example of figure 4, the point shown represents a typical space coordinate midway between two adjacent trajectories, in this case, trajectories 5 and 6. The normal distance between the trajectories at this point is d . The area of the annulus is then

$$A = 2\pi r d = 2\pi \bar{\rho}_{5,j} \sin \bar{\theta}_{5,j} d \quad (20)$$

The general expression for the current density, $J = I/A$ (eq. (17a)), may now be written as

$$J_{i,j} = \frac{(2i - 1)J_0 d A_1}{2\pi (\bar{\rho}_{i,j} \sin \bar{\theta}_{i,j}) d_{i,j}} \quad (21a)$$

or

$$J_{i,j} = \frac{(2i - 1)r_2^2 J_0}{2d_{i,j}(\bar{\rho}_{i,j} \sin \bar{\theta}_{i,j})} \quad (21b)$$

Notice that current is preserved in each annular region, namely

$$I_{0,i} = (2i - 1)J_0 d A_1 = J_{i,j} A_{i,j} \quad (22)$$

Since $A_{i,j}$ can be computed at $(\bar{\rho}_{i,j}, \bar{\theta}_{i,j})$ by

$$A_{i,j} = 2\pi \bar{\rho}_{i,j} \sin \bar{\theta}_{i,j} d_{i,j} \quad (23)$$

where $d_{i,j}$ is the normal thickness of an annulus at this point.

Use of Irregular Mesh Spacing

The successful solution to this problem, especially those phases dealing with high current densities, was largely due to the use of irregular mesh spacing in both the ρ and θ directions. From figure 5 it is clearly apparent that the region in which the solution varies most rapidly is immediately along and adjacent to the negative polar axis, where the entering electron beam is most dense and of greatest velocity. Consequently, a closely spaced mesh was used in this region. Conversely, a coarse spacing was used where the solution was varying very slowly and quite predictably.

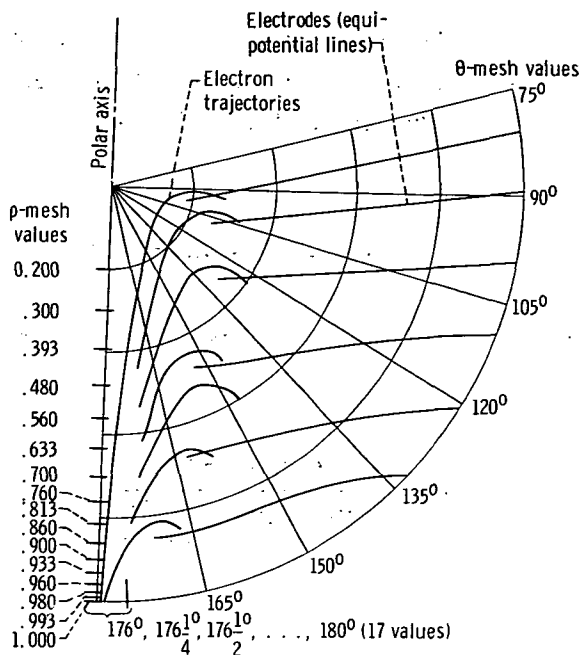


Figure 5. - Cross section of right half of spherical cone-shaped collector, showing typical pattern of electrodes, electron trajectories, and irregular mesh spacing in both the ρ and θ directions.

Convergence Acceleration

Experience has shown that in solving this problem, the iterants are well behaved and ultimately converge to an acceptable approximation to the solution. But because of the steadily decaying oscillatory nature of the iterants, a considerable savings in computer execution time was achieved by halving the newly calculated changes in the variables at each step. Normally, a maximum of five iterations would provide an acceptable solution.

FORTRAN PROGRAM

General Description

The program consists of the following 16 subroutines:

(1) MAIN is the executive routine for processing multiple cases and has primary control of logical flow throughout the complete program.

(2) INPUT reads and prints initial conditions, parameters, and other data required for internal use by the program (printout frequency, looping indices, convergence criteria, etc.).

(3) INTGRN controls integration looping of equations of motion, step size, change-over of coordinate systems, and the number of iterations required for convergence.

(4) DE is the spherical coordinate version of a routine for computing trajectories by integrating the equations of motion.

(5) DERIV calculates $\partial V/\partial \rho$ and $\partial V/\partial \theta$ for any specified interior point.

(6) RK is the spherical coordinate version of a Runge-Kutta integration subroutine used to compute trajectories.

(7) MESH generates graduated mesh point arrays in both the r and θ directions for any specified collector geometry.

(8) RZTRAJ is the cylindrical coordinate version of a routine for computing trajectories by integrating equations of motion.

(9) RZRK is the cylindrical coordinate version of a Runge-Kutta integration subroutine used to compute trajectories.

(10) RZDE contains the equations of motion in the cylindrical coordinate system. It is similar to subroutine DE.

(11) OUT controls the printing of results at specified intervals along the trajectories.

(12) VFIELD provides for the calculation of the potential field for any particular set of boundary values and source terms. It uses the program described in reference 2.

(13) EQLINE calculates the spherical coordinates of any specified number of equipotential lines. It is used only after convergence is achieved in the main portion of the program.

(14) RHSCAL generates space charge values along center lines of the various annuli formed by the trajectories. It interpolates for these values at each mesh point, as required in the solution of Poisson's equation.

(15) PSICAL calculates the magnetic flux ψ of the magnetic field at each mesh point.

(16) BRBZ calculates B_r and B_z , the r and z components of the magnetic field, at each mesh point.

All calculations were done on the IBM 7094 II/7044 Direct Couple System computer. The program will perform about 210 integration steps per minute. This figure is based on trajectory calculations for eight electron energy groups.

About 15 000 storages are required for the program. This does not include that required for the solution of Poisson's equation. An additional 10 000 storage locations are needed for a solution to Poisson's equation similar to that described in reference 2.

The FORTRAN program is listed in appendix B, FORTRAN symbols are defined in appendix C, and flow charts are presented in appendix D.

Using the Program

The program always starts by reading in a nine-card input data deck. The contents of each of these cards is now described.

Card 1 (Format 55H. . .)

Contains any desired information to identify the particular case being run (card columns 1 to 55 only). This will be printed out at the top of a listing.

Card 2 (Format 4E10.3)

R radius of collector, R, cm
B0 magnetic flux density, B_0 , G
DTHTD θ step size used in Runge-Kutta integration (spherical coordinate),
 $\Delta\theta$, deg
TH1 cone angle, θ_1 , deg

Card 3 (Format 8E10.3)

ZI0 initial current¹, I_0 , A
ZJ0 current density¹, J_0 , A/cm²
V0 initial electric potential, V_0 , V
DELR r step size used in Runge-Kutta integration (cylindrical coordinates), Δr
CONFLO indicates confined flow when equal to 1 and Brillouin flow when equal to 0
RAD radius of collector entry hole, a, cm
FLOOP number of iterations for space charge calculations (If no space charge calculation is desired, this value should be set to 1.)

Card 4 (Format 40I2)

NT number of trajectories to be calculated
KPOI printout frequency control, (e.g., 4 means to print results at every fourth integration step of a trajectory)
N1 }
N2 }
N3 } integrate trajectories N1 to N2 in steps of N3

¹These two values are used only in the calculation of the source term in Poisson's equation when space charge iteration is necessary.

IBAR when nonzero, indicates boundary values will be supplied along the negative polar axis
LOOP counter for number of space charge loops
KPOSC print control for interim space charge calculations

Card 5 (Format 4F5.1)

These values are used by the integration subroutine in the spherical coordinate system, which is the system used in the beginning portion of the program.

THSFAC } step-size controls; increase step size DTH by a factor of THSFAC
THSDEL } every THSDEL (deg) in the θ_5 range from THSWHI (deg) to
THSWHI } THSWLO (deg)
THSWLO }

Card 6 (Format 16F5.3)

VSMI(I), electron energy classes for each of NT trajectories to be solved
I = 1, NT for

Card 7 (Format I2, 10F5.3)

This calculation is done only once, after convergence has been achieved in the main part of the program.

NEQL number of equipotential lines to be calculated
EQL(I), array of potential values for each equipotential line
I = 1, NEQL

Card 8 (Format 16F5.3)

XT(J, 16), boundary values on surface of spherical collector from initial
J = 1, 16 cone angle θ_1 to 180^0 , V

Card 9 (Format 16F5.3)

XT(J, 16) continuation of card 8
J = 17, JF

Two sample test runs are given in appendix A. These runs were chosen to more clearly illustrate the makeup of the input data deck and to show the various options in output format available to the user.

CONCLUDING REMARKS

We have described the numerical technique used to obtain a solution to a problem

associated with the design of an axisymmetric, spherical, depressed collector. Varying initial conditions include current density of electrons, surface potential on the collector, collector geometry, and the velocity and position of entering electron groups.

Of particular importance to the successful solution is the scheme used near the entry hole in the collector. Here the entering electron stream is of highest velocity and greatest density, giving rise to computational problems, especially in cases of high initial current densities.

Calculations by others in the past were successful in handling current densities to 50 A/cm^2 before numerical difficulties precluded further computation. The numerical approach described in this report is used to solve systems with current densities to 100 A/cm^2 .

Computational stability was achieved primarily by using a graduated mesh in both the r and θ directions, with greatest mesh point density in the hole region. In addition, computational efficiency was improved by taking advantage of the fact that all entering electron groups were distributed uniformly both in positioning and velocity grouping. That is, the fastest group entered closest to the axis, and the slowest group entered nearest the edge of the entry hole.

Space charge effects were found to be negligible for initial current densities less than 10 A/cm^2 . Consequently, the problem was reduced to requiring only one iteration and essentially solving Laplace's equation to obtain the potential distribution inside the collector.

Lewis Research Center,
National Aeronautics and Space Administration,
Cleveland, Ohio, June 2, 1972,
111-05.

APPENDIX A

SAMPLE PROBLEMS

Short, partial, representative computer output listings of two sample runs are presented. Run 1, depicted graphically in figure 6, is for a 0.2 spike, no space charge iterations, confined flow, and a cone angle of 60° . Run 2, figure 7, is for no spike, space charge effects calculated, Brillouin flow, and a cone angle of 45° .

Figure 7 shows a poor pattern. Beam spread and separation is rather nonuniform and erratic. In contrast, figure 6 shows well-shaped and well-behaved beams with good spread and uniform spacing.

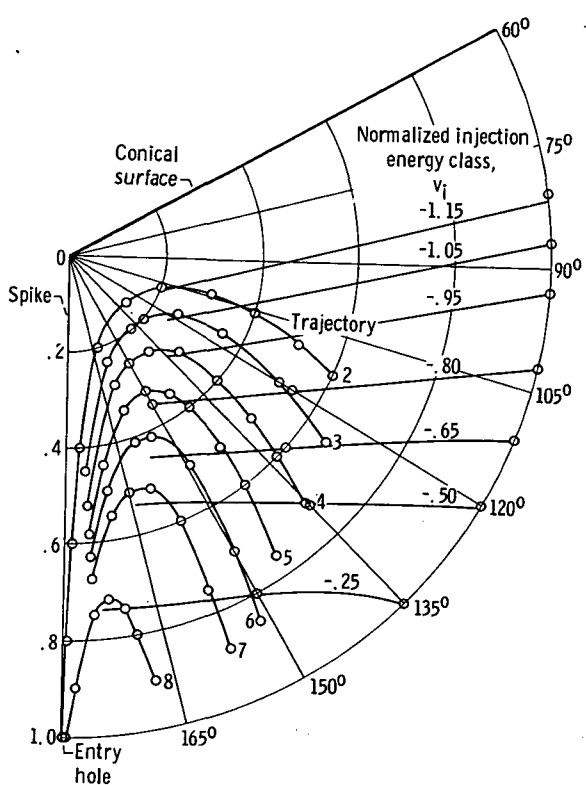


Figure 6. - Sample run 1. No iterations necessary (current density, 8 A/cm^2 ; 0.2 spoke; cone angle, 60°).

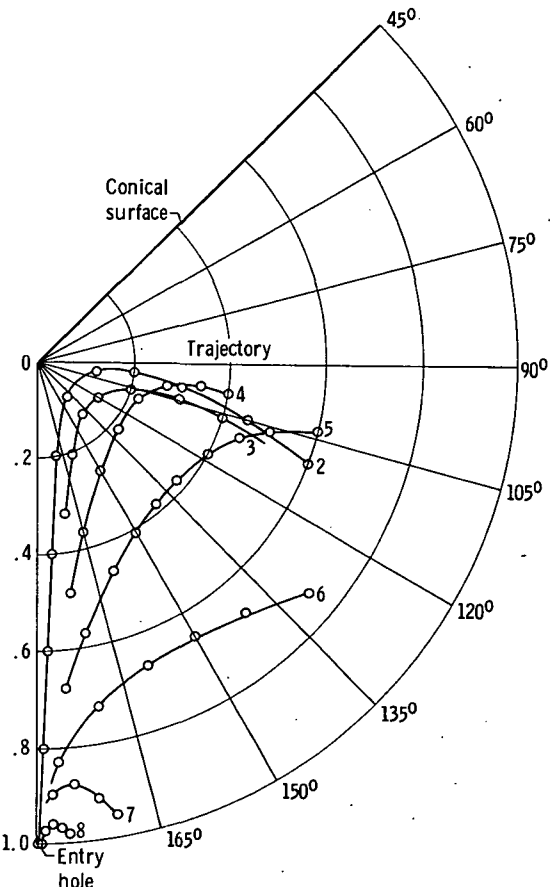


Figure 7. - Sample run 2. Five iterations for space charge effect; no spike; cone angle, 45° .

Sample Run 1

SAMPLE RUN NO. 1

NO SPACE CHARGE EFFECTS
CONFINED FLOW.

INPUT-

$F_0 = 8.860E-14$ $K_P = 6.158E-07$
 $\text{EMPGAE} = 1.414E+10$ $\text{ETAC} = 1.753E+15$
 $I_0 = 4.000E-01$
 $J_0 = 2.050E+00$ $R = 8.000E+00$
 $V_0 = 7.500E+03$ $R_0 = 1.000E-06$
 $\text{TAU02} = 0.243E-17$ $\text{RAD} = 0.400E+00$

CUTPLT EVERY 4 STEPS.

INITIAL VALUES-

I	DELT	DELI	THETA	VSM	VI	INJEC.	PSIO
	(RAD)	(DEG)	(DEG)			ANGLES	
2	0.076	0.358	179.642	0.900	6.75E+03	2.000	3.925E-09
3	0.013	0.716	179.284	0.800	6.00E+03	3.000	1.568E-08
4	0.019	1.074	178.926	0.700	5.25E+03	4.000	3.517E-08
5	0.025	1.433	178.567	0.600	4.50E+03	5.000	6.225E-08
6	0.031	1.791	178.209	0.500	3.75E+03	6.000	9.659E-08
7	0.038	2.149	177.851	0.400	3.00E+03	7.000	1.373E-07
8	0.044	2.507	177.493	0.200	1.50E+03	8.000	1.809E-07

EAR VALUES-

R	V
0.0	-1.500
0.200	-1.500
0.300	-0.782
0.393	-0.625
0.480	-0.503
0.560	-0.411
0.633	-0.327
0.700	-0.260
0.760	-0.198
0.813	-0.148
0.860	-0.104
0.900	-0.076
0.933	-0.048
0.960	-0.028
0.980	-0.014
0.993	-0.005
1.000	0.

POTENTIAL FIELD

INPUT-

THTA	0.560	0.633	0.700	0.760	0.813	0.860	0.900	0.933	0.960	0.980	0.993	1.000
60.00	-1.50E+00											
75.00	0.	0.	0.	0.	0.	0.	0.	0.	0.	0.	0.	-1.25E+00
90.00	0.	0.	0.	0.	0.	0.	0.	0.	0.	0.	0.	-1.00E+00
105.00	0.	0.	0.	0.	0.	0.	0.	0.	0.	0.	0.	-7.50E-01
120.00	0.	0.	0.	0.	0.	0.	0.	0.	0.	0.	0.	-5.00E-01
135.00	0.	0.	0.	0.	0.	0.	0.	0.	0.	0.	0.	-2.50E-01
150.00	0.	0.	0.	0.	0.	0.	0.	0.	0.	0.	0.	-1.00E-01
165.00	0.	0.	0.	0.	0.	0.	0.	0.	0.	0.	0.	-5.00E-02
176.00	0.	0.	0.	0.	0.	0.	0.	0.	0.	0.	0.	-2.50E-02
176.25	0.	0.	0.	0.	0.	0.	0.	0.	0.	0.	0.	-1.25E-02
176.50	0.	0.	0.	0.	0.	0.	0.	0.	0.	0.	0.	-6.25E-03
176.75	0.	0.	0.	0.	0.	0.	0.	0.	0.	0.	0.	-3.125E-03
177.00	0.	0.	0.	0.	0.	0.	0.	0.	0.	0.	0.	-1.5625E-03
177.25	0.	0.	0.	0.	0.	0.	0.	0.	0.	0.	0.	-7.8125E-04
177.50	0.	0.	0.	0.	0.	0.	0.	0.	0.	0.	0.	-3.90625E-04
177.75	0.	0.	0.	0.	0.	0.	0.	0.	0.	0.	0.	-1.953125E-04
178.00	0.	0.	0.	0.	0.	0.	0.	0.	0.	0.	0.	-9.765625E-05
178.25	0.	0.	0.	0.	0.	0.	0.	0.	0.	0.	0.	-4.8828125E-05
178.50	0.	0.	0.	0.	0.	0.	0.	0.	0.	0.	0.	-2.44140625E-05
178.75	0.	0.	0.	0.	0.	0.	0.	0.	0.	0.	0.	-1.220703125E-05
179.00	0.	0.	0.	0.	0.	0.	0.	0.	0.	0.	0.	-6.103515625E-06
179.25	0.	0.	0.	0.	0.	0.	0.	0.	0.	0.	0.	-3.0517578125E-06
179.50	0.	0.	0.	0.	0.	0.	0.	0.	0.	0.	0.	-1.52587890625E-06
179.75	0.	0.	0.	0.	0.	0.	0.	0.	0.	0.	0.	-7.62939453125E-07
180.00	-4.11E-01	-3.27E-01	-2.60E-01	-1.98E-01	-1.48E-01	-1.08E-01	-7.57E-02	-4.80E-02	-2.80E-02	-1.40E-02	-4.60E-03	0.

x1=-1.50

POTENTIAL FIELD

OUTPUT-

THTA	0.200	0.300	0.393	0.480	0.560	0.633	0.700	0.760	0.813	0.860	0.900	0.933	0.960	0.980	0.993	1.000
40.00	-1.5000	-1.5000	-1.5000	-1.5000	-1.5000	-1.5000	-1.5000	-1.5000	-1.5000	-1.5000	-1.5000	-1.5000	-1.5000	-1.5000	-1.5000	
75.00	-1.3834	-1.3515	-1.3273	-1.3086	-1.2939	-1.2824	-1.2734	-1.2666	-1.2614	-1.2575	-1.2528	-1.2515	-1.2502	-1.2500	-1.2500	
90.00	-1.0000	-1.2819	-1.2268	-1.1739	-1.1368	-1.1071	-1.0822	-1.0638	-1.0481	-1.0355	-1.0254	-1.0175	-1.0113	-1.0066	-1.0000	
105.00	-1.1946	-1.1058	-1.0366	-0.9807	-0.9347	-0.8960	-0.8648	-0.8384	-0.8165	-0.7984	-0.7837	-0.7730	-0.7630	-0.7564	-0.7521	-0.7500
120.00	-1.1227	-1.074	-0.9161	-0.8448	-0.7774	-0.7233	-0.6772	-0.6380	-0.6047	-0.5769	-0.5539	-0.5354	-0.5210	-0.5104	-0.5034	-0.5000
135.00	-1.0690	-0.9279	-0.8157	-0.7216	-0.6404	-0.5695	-0.5074	-0.4530	-0.4058	-0.3654	-0.3315	-0.3037	-0.2820	-0.2659	-0.2553	-0.2500
150.00	-1.0390	-0.8706	-0.7399	-0.6301	-0.5342	-0.4487	-0.3716	-0.3018	-0.2388	-0.1823	-0.1326	-0.0898	-0.0547	-0.0276	-0.0093	0.
165.00	-1.0470	-0.8378	-0.6917	-0.5727	-0.4708	-0.3819	-0.3424	-0.2369	-0.1793	-0.1308	-0.0910	-0.0591	-0.0347	-0.0170	-0.0056	0.
176.00	-1.1201	-0.8251	-0.6692	-0.5674	-0.4454	-0.3573	-0.2816	-0.2169	-0.1625	-0.1176	-0.0781	-0.0526	-0.0338	-0.0151	-0.0050	0.
176.25	-1.1251	-0.8246	-0.6685	-0.5467	-0.4448	-0.3567	-0.2811	-0.2165	-0.1622	-0.1174	-0.0811	-0.0525	-0.0337	-0.0151	-0.0050	0.
176.50	-1.1304	-0.8240	-0.6677	-0.5459	-0.4441	-0.3562	-0.2807	-0.2161	-0.1619	-0.1172	-0.0810	-0.0524	-0.0337	-0.0150	-0.0049	0.
176.75	-1.1362	-0.8233	-0.6670	-0.5451	-0.4435	-0.3556	-0.2802	-0.2157	-0.1616	-0.1169	-0.0808	-0.0523	-0.0326	-0.0150	-0.0049	0.
177.00	-1.1425	-0.8220	-0.6661	-0.5443	-0.4428	-0.3550	-0.2797	-0.2153	-0.1613	-0.1167	-0.0837	-0.0522	-0.0305	-0.0150	-0.0049	0.
177.25	-1.1493	-0.8218	-0.6653	-0.5434	-0.4421	-0.3543	-0.2792	-0.2149	-0.1609	-0.1165	-0.0805	-0.0521	-0.0305	-0.0149	-0.0049	0.
177.50	-1.1566	-0.8210	-0.6643	-0.5425	-0.4413	-0.3536	-0.2787	-0.2145	-0.1606	-0.1162	-0.0803	-0.0520	-0.0304	-0.0149	-0.0049	0.
177.75	-1.1652	-0.8200	-0.6633	-0.5414	-0.4404	-0.3529	-0.2782	-0.2140	-0.1602	-0.1160	-0.0802	-0.0519	-0.0303	-0.0149	-0.0049	0.
178.00	-1.1745	-0.8180	-0.6622	-0.5403	-0.4395	-0.3521	-0.2776	-0.2135	-0.1598	-0.1157	-0.0800	-0.0517	-0.0303	-0.0148	-0.0049	0.
178.25	-1.1851	-0.8178	-0.6616	-0.5390	-0.4385	-0.3512	-0.2769	-0.2129	-0.1594	-0.1154	-0.0798	-0.0516	-0.0302	-0.0148	-0.0049	0.
178.50	-1.1974	-0.8164	-0.6594	-0.5375	-0.4374	-0.3502	-0.2762	-0.2123	-0.1589	-0.1150	-0.0796	-0.0514	-0.0301	-0.0148	-0.0049	0.

178.75-1.2120-0.8148-0.6577-0.5358-0.4361-0.3490-0.2754-0.2116-0.1583-C.1147-0.3794-C.0513-0.3307-0.2147-0.0048 C.
 179.60-1.2298-0.8128-0.6557-0.5338-0.4345-0.3476-0.2744-0.2108-0.1577-0.1142-0.3791-C.0511-0.3299-C.1147-0.0048 C.
 179.25-1.2528-0.8102-0.6530-0.5311-0.4324-0.3459-0.2731-C.2097-0.1568-0.1137-0.3788-C.0518-C.2297-0.2146-0.0048 C.
 179.50-1.2850-0.8075-0.6494-0.5274-0.4296-0.3434-0.2714-C.2082-0.1557-0.1129-0.3784-C.0504-C.2295-C.1145-0.0048 C.
 179.75-1.3387-0.8004-0.6433-0.5213-0.4249-0.3393-0.2685-0.2058-C.1537-0.1116-0.0777-0.0498-0.0291-C.1144-0.0048 C.
 180.60-1.5000-C.7820-0.6250-0.5213-0.4249-0.3393-0.2685-0.2058-C.1537-C.1116-0.3777-0.0498-C.0291-C.1144-0.0047 C.

TABLE OF RHO-VALUES FOR EQUIPOTENTIAL LINES

THFTA	-0.90	-0.80	-0.70	-0.60	-0.50	-0.40	-0.30	-0.20	-0.10
60.00	0.	0.	0.	0.	0.	0.	0.	0.	0.
75.00	0.	0.	0.	0.	0.	0.	0.	0.	0.
90.00	0.	0.	0.	0.	0.	0.	0.	0.	0.
105.00	0.627	0.856	0.	0.	0.	0.	0.	0.	0.
120.00	0.412	0.531	0.667	0.821	1.000	0.	0.	0.	0.
135.00	0.323	0.408	0.511	0.602	0.708	0.820	0.938	0.	0.
150.00	0.283	0.350	0.425	0.505	0.589	0.675	0.762	0.845	0.925
165.00	0.270	0.324	0.388	0.460	0.537	0.618	0.704	0.794	0.891
176.00	0.275	0.315	0.375	0.443	0.517	0.598	0.684	0.777	0.879
176.50	0.275	0.315	0.374	0.442	0.517	0.597	0.683	0.776	0.879
176.75	0.275	0.314	0.374	0.442	0.516	0.597	0.683	0.775	0.879
177.00	0.276	0.313	0.373	0.440	0.515	0.596	0.682	0.775	0.879
177.25	0.276	0.313	0.373	0.440	0.514	0.595	0.682	0.775	0.878
177.50	0.276	0.312	0.372	0.439	0.514	0.595	0.681	0.774	0.878
177.75	0.277	0.312	0.371	0.438	0.513	0.594	0.681	0.774	0.878
178.00	0.277	0.311	0.371	0.438	0.512	0.593	0.680	0.773	0.878
178.25	0.278	0.311	0.370	0.437	0.511	0.592	0.679	0.773	0.877
178.50	0.278	0.310	0.369	0.436	0.510	0.591	0.679	0.772	0.877
178.75	0.279	0.309	0.368	0.434	0.509	0.590	0.678	0.772	0.877
179.00	0.279	0.308	0.367	0.433	0.507	0.589	0.677	0.771	0.876
179.25	0.280	0.306	0.365	0.431	0.505	0.587	0.675	0.770	0.876
179.50	0.280	0.304	0.363	0.428	0.502	0.585	0.673	0.768	0.875
179.75	0.281	0.300	0.360	0.424	0.498	0.581	0.670	0.766	0.874
180.00	0.284	0.297	0.349	0.414	0.498	0.581	0.670	0.766	0.874

DELTHTFA=-0.0200 DEG.

TRJ	THFTA	RHO	VT	DVDRH	DVDTH	RH-PR	RH-PPR	THD2	PHD2	PSI
STEP 0										
2	179.64	1.000	0.	0.	0.	2.408E+01	1.145E+03	6.366E+16	1.470E+12	3.914E-29
3	179.28	1.000	0.	0.	0.	1.531E+01	4.606E+02	1.396E+15	1.538E+12	1.563E-28
4	178.93	1.000	-0.	-0.	C.	1.122E+01	2.461E+02	2.267E+15	1.667E+12	3.927E-28
5	178.57	1.000	-0.	-0.	0.	8.842E+00	1.520E+02	3.113E+15	1.896E+12	6.206E-28
6	178.21	1.000	-0.	-0.	0.	7.290E+00	1.023E+02	3.794E+15	2.350E+12	9.625E-28
7	177.85	1.000	-0.	-0.	0.	6.196E+00	7.236E+01	4.172E+15	3.528E+12	1.367E-27
8	177.49	1.000	-0.	-0.	0.	5.382E+00	4.759E+01	2.743E+15	7.775E+12	1.797E-27
STEP 4										
2	179.56	0.967	-2.414E-02	5.592E+03	0.	2.317E+01	5.301E+02	6.694E+14	2.790E+16	1.830E-09
3	179.20	0.979	-1.554E-02	5.671E+03	0.	1.509E+01	-2.860E+01	1.404E+15	2.244E+16	9.319E-09
4	178.85	0.984	-1.147E-02	5.546E+03	0.	1.113E+01	-8.148E+01	2.267E+15	1.660E+16	2.355E-08
5	178.49	0.988	-5.097E-03	5.573E+03	0.	8.801E+00	-7.892E+01	3.095E+15	1.352E+16	4.413E-08
6	178.13	0.990	-7.539E-03	5.595E+03	0.	7.278E+00	-7.366E+01	3.750E+15	1.257E+16	6.974E-08
7	177.77	0.991	-6.441E-03	5.615E+03	0.	6.210E+00	-6.643E+01	4.089E+15	1.436E+16	9.643E-08
8	177.41	0.992	-5.646E-03	5.633E+03	0.	5.459E+00	-5.137E+01	2.593E+15	2.361E+16	1.102E-07
STEP 8										
2	179.48	0.935	-4.686E-02	5.897E+03	0.	2.269E+01	9.558E+02	7.155E+14	3.651E+16	7.893E-12
3	179.12	0.958	-3.160E-02	5.949E+03	0.	1.504E+01	1.546E+02	1.391E+15	4.761E+16	4.933E-09
4	178.77	0.969	-2.331E-02	5.724E+03	0.	1.124E+01	-4.931E+01	2.182E+15	4.321E+16	1.440E-08
5	178.41	0.975	-1.483E-02	5.754E+03	0.	8.936E+00	-8.828E+01	2.957E+15	3.827E+16	2.929E-08
6	178.05	0.980	-1.521E-02	5.779E+03	0.	7.400E+00	-8.199E+01	3.574E+15	3.552E+16	4.852E-08
7	177.69	0.983	-1.299E-02	5.619E+03	0.	6.295E+00	-5.407E+01	3.916E+15	3.486E+16	7.017E-08
8	177.33	0.985	-1.139E-02	5.637E+03	0.	5.457E+00	1.168E+01	2.518E+15	3.577E+16	8.977E-08
STEP 12										
2	179.40	0.906	-7.391E-02	6.253E+03	0.	2.065E+01	1.049E+03	7.943E+14	2.933E+16	4.148E-10
3	179.04	0.937	-4.816E-02	5.959E+03	0.	1.467E+01	3.465E+02	1.429E+15	5.311E+16	2.751E-09
4	178.69	0.953	-3.558E-02	5.991E+03	0.	1.122E+01	8.068E+01	2.152E+15	5.774E+16	8.831E-09
5	178.33	0.963	-2.808E-02	5.760E+03	0.	9.012E+00	-1.634E+01	2.860E+15	5.618E+16	1.933E-08
6	177.97	0.969	-2.324E-02	5.784E+03	0.	7.486E+00	-3.894E+01	3.436E+15	5.425E+16	3.358E-08
7	177.61	0.974	-1.977E-02	5.804E+03	0.	6.348E+00	-2.491E+01	3.786E+15	5.260E+16	5.061E-08
8	177.25	0.977	-1.720E-02	5.823E+03	0.	5.467E+00	-1.826E+01	2.432E+15	4.562E+16	7.342E-08
STEP 16										
2	179.32	0.978	-5.866E-02	6.515E+03	0.	1.921E+01	9.979E+02	8.907E+14	2.194E+16	2.587E-10
3	178.96	0.917	-6.500E-02	6.316E+03	0.	1.411E+01	4.349E+02	1.509E+15	4.920E+16	1.688E-09
4	178.61	0.937	-4.806E-02	5.958E+03	0.	1.104E+01	1.755E+02	2.182E+15	6.105E+16	5.676E-09
5	178.25	0.950	-3.811E-02	6.023E+03	0.	8.980E+00	5.802E+01	2.830E+15	6.438E+16	1.311E-08
6	177.89	0.959	-3.139E-02	6.044E+03	0.	7.506E+00	1.116E+01	3.361E+15	6.479E+16	2.379E-08
7	177.53	0.965	-2.666E-02	5.809E+03	0.	6.364E+00	2.516E+00	3.700E+15	6.474E+16	3.644E-08
8	177.17	0.969	-2.315E-02	5.827E+03	0.	5.485E+00	-3.021E+00	2.338E+15	6.183E+16	5.045E-08
STEP 20										
2	179.24	0.852	-1.212E-01	6.939E+03	C.	1.788E+01	9.212E+02	9.991E+14	1.650E+16	1.814E-10
3	178.88	0.898	-8.141E-02	6.557E+03	0.	1.349E+01	4.578E+02	1.615E+15	4.300E+16	1.132E-09

SWITCH TO R-Z COORDINATE SYSTEM-
TRAJECTORY NO. 4 DELR=0.010

THETA	RHO	R	Z	DVDR	DVDZ	ZP	ZPP	V
167.39	0.388	0.085	-0.379	1.346E-01	-1.591E+00	1.836E-01	-2.520E+02	-6.967E-01
166.59	0.408	0.095	-0.397	1.097E-01	-1.388E+00	-3.808E+00	-2.384E+02	-6.684E-01
166.75	0.457	0.105	-0.445	1.153E-01	-1.387E+00	-5.494E+00	-1.190E+02	-6.014E-01
167.20	0.518	0.115	-0.505	9.988E-02	-1.284E+00	-6.669E+00	-7.624E+01	-5.207E-01
167.72	0.586	0.125	-0.573	9.760E-02	-1.218E+00	-7.083E+00	-5.065E+01	-4.342E-01
168.22	0.660	0.135	-0.646	1.015E-01	-1.162E+00	-7.488E+00	-3.238E+01	-3.458E-01
168.67	0.737	0.145	-0.722	1.113E-01	-1.111E+00	-7.729E+00	-1.723E+01	-2.580E-01
169.06	0.815	0.155	-0.800	1.166E-01	-1.014E+00	-7.844E+00	-5.895E+00	-1.730E-01
169.38	0.894	0.165	-0.879	1.359E-01	-9.620E-01	-7.840E+00	5.332E+00	-9.392E-02
169.65	0.973	0.175	-0.957	1.424E-01	-8.405E-01	-7.754E+00	1.205E+01	-2.276E-02
169.87	1.050	0.185	-1.034	1.627E-01	-8.097E-01	-7.607E+00	1.701E+01	4.139E-02

STEP 380
 2 168.02 0.275 -8.922E-01 1.699E+04 -2.550E+02 -7.912E-02 1.261E+01 3.917E+16 2.703E+13 4.377E-11
 3 167.66 0.325 -7.953E-01 1.188E+04 4.398E+02 1.515E-01 2.084E+01 1.513E+16 1.977E+14 7.952E-11
 STEP 384
 2 167.86 0.275 -6.915E-01 1.652E+04 -2.484E+02 -1.124E-01 1.183E+01 3.953E+16 2.554E+13 4.502E-11
 3 167.50 0.325 -7.960E-01 1.187E+04 4.388E+02 9.171E-02 2.200E+01 1.456E+16 1.887E+14 8.117E-11
 STEP 388
 2 167.70 0.275 -8.906E-01 1.665E+04 -2.396E+02 -1.452E-01 1.17CE+01 3.982E+16 2.411E+13 4.634E-11
 3 167.34 0.325 -7.964E-01 1.186E+04 4.383E+02 2.838E+02 2.339E+01 1.395E+16 1.798E+14 8.299E-11

SWITCH TO R-Z COORDINATE SYSTEM-
 TRAJECTORY NO. 3 DELR=.010

THETA	RHO	R	Z	DVDR	DVDZ	ZP	ZPP	V
167.26	0.325	0.072	-0.317	1.733E-01	-1.582E+00	2.104E-01	-2.412E+02	-7.965E-01
166.18	0.342	0.082	-0.332	1.506E-01	-1.574E+00	-2.982E+00	-1.719E+02	-7.711E-01
166.03	0.380	0.092	-0.368	1.737E-01	-1.577E+00	-4.195E+00	-8.929E+01	-7.116E-01
166.22	0.427	0.102	-0.414	1.223E-01	-1.386E+00	-4.956E+00	-6.387E+01	-6.440E-01
166.55	0.480	0.112	-0.467	1.004E-01	-1.286E+00	-5.507E+00	-4.997E+01	-5.701E-01
166.94	0.538	0.122	-0.524	1.125E-01	-1.282E+00	-5.936E+00	-3.653E+01	-4.954E-01
167.32	0.600	0.132	-0.585	1.106E-01	-1.216E+00	-6.280E+00	-2.759E+01	-4.186E-01
167.69	0.664	0.142	-0.649	1.141E-01	-1.162E+00	-6.495E+00	-1.981E+01	-3.415E-01
168.02	0.731	0.152	-0.715	1.220E-01	-1.112E+00	-6.655E+00	-1.270E+01	-2.653E-01
168.32	0.799	0.162	-0.762	1.332E-01	-1.062E+00	-6.752E+00	-6.234E+00	-1.914E-01
168.58	0.867	0.172	-0.850	1.386E-01	-9.669E-01	-6.787E+00	-8.964E+01	-1.209E-01
168.80	0.935	0.182	-0.918	1.477E-01	-8.795E-01	-6.772E+00	3.81CE+00	-5.565E-02
168.99	1.004	0.192	-0.985	1.601E-01	-8.159E-01	-6.715E+00	7.435E+00	3.03CE-03

SWITCH TO R-Z COORDINATE SYSTEM-
 TRAJECTORY NO. 2 DELR=.010

THETA	RHO	R	Z	DVDR	DVDZ	ZP	ZPP	V
167.58	0.276	0.059	-0.269	5.909E-01	-2.163E+00	-3.479E-01	-1.075E+02	-8.898E-01
165.95	0.286	0.069	-0.277	5.171E-01	-2.038E+00	-1.088E+00	-5.181E+01	-8.680E-01
164.71	0.301	0.079	-0.290	8.156E-03	-1.617E+00	-1.529E+00	-4.258E+01	-8.371E-01
163.81	0.320	0.089	-0.368	1.875E-02	-1.611E+00	-1.949E+00	-4.147E+01	-8.089E-01
163.21	0.344	0.099	-0.329	2.845E-02	-1.608E+00	-2.359E+00	-4.063E+01	-7.740E-01
162.88	0.371	0.109	-0.355	1.629E-02	-1.609E+00	-2.764E+00	-4.034E+01	-7.326E-01
162.76	0.403	0.119	-0.384	-4.307E-02	-1.434E+00	-3.168E+00	-4.056E+01	-6.864E-01
162.82	0.438	0.129	-0.418	-3.963E-02	-1.433E+00	-3.579E+00	-4.157E+01	-6.385E-01
163.01	0.477	0.139	-0.456	-3.965E-02	-1.433E+00	-4.001E+00	-4.290E+01	-5.846E-01
163.32	0.520	0.149	-0.498	-6.120E-02	-1.340E+00	-4.442E+00	-4.495E+01	-5.283E-01
163.70	0.568	0.159	-0.545	-7.246E-02	-1.286E+00	-4.901E+00	-4.723E+01	-4.669E-01
164.15	0.620	0.169	-0.596	-6.173E-02	-1.275E+00	-5.378E+00	-4.828E+01	-4.019E-01
164.64	0.677	0.179	-0.653	-5.701E-02	-1.223E+00	-5.867E+00	-4.866E+01	-3.329E-01
165.14	0.738	0.189	-0.714	1.827E-01	-1.112E+00	-6.270E+00	1.057E+00	-2.610E-01
165.60	0.801	0.199	-0.776	1.873E-01	-1.065E+00	-6.252E+00	3.005E+00	-1.914E-01
165.99	0.864	0.209	-0.839	1.848E-01	-9.747E-01	-6.215E+00	4.456E+00	-1.256E-01
166.31	0.927	0.219	-0.901	1.954E-01	-9.267E-01	-6.158E+00	6.441E+00	-6.471E-02
166.59	0.989	0.229	-0.962	1.924E-01	-8.249E-01	-6.088E+00	7.400E+00	-9.440E-03
166.82	1.050	0.239	-1.022	2.100E-01	-8.192E-01	-6.007E+00	8.701E+00	4.229E-02

Sample Run 2

SAMPLE RUN NO. 2
 5 ITERATIONS FOR SPACE
 CHARGE EFFECTS
 BRILLOUIN FLOW
 INPUT-

EC = 8.86CE-14 KP = 1.160E-07
 OMEGA= 1.414E+10 ETA0= 1.753E+15

IC= 8.3CE-02
 JO= 8.0CE+01 P = 8.00CE+00

VO= 8.00CE+03 RO = 1.00CE-06

TAU2C2= 0.228E-17 RAD = 0.100E+00

OUTPUT EVERY 6 STEPS.

I	DELI	DELI	THETA	VSM	VI	INJEC.	PSIG
	(RAD)	(DEG)	(DEG)			ANGLES	
2	0.002	0.000	179.920	0.920	7.20E+03	2.000	C.
3	0.003	0.179	179.821	0.820	6.40E+03	3.000	C.
4	0.005	0.269	179.731	0.720	5.60E+03	4.000	C.
5	0.006	0.358	179.642	0.620	4.80E+03	5.000	C.
6	0.008	0.443	179.552	0.520	4.00E+03	6.000	C.
7	0.009	0.537	179.463	0.420	3.20E+03	7.000	C.
8	0.011	0.627	179.373	0.220	2.60E+03	8.000	C.

END OF RUN

POTENTIAL FIELD

INPUT-	RHO
THETA	0.560
45.00	0.673
-1.00E+00	-0.700
-1.00E+00	-0.760
-1.00E+00	0.813
-1.00E+00	0.860
-1.00E+00	0.900
-1.00E+00	0.933
-1.00E+00	0.960
-1.00E+00	0.980
-1.00E+00	0.993
-1.00E+00	1.000
60.00	0.
60.00	0.
75.00	0.
75.00	0.
90.00	0.
105.00	0.
120.00	0.
135.00	0.
150.00	0.
165.00	0.
175.25	0.
175.50	0.
176.75	0.
177.00	0.
177.25	0.
177.50	0.
177.75	0.
178.00	0.
178.25	0.
178.50	0.
178.75	0.
179.00	0.
179.25	0.
179.50	0.
179.75	0.
180.00	0.

X1=-1.00)

POTENTIAL FIELD

OUTPUT-	RHC
THETA	0.200
45.00-1	0.300
60.00-0	0.393
75.00-0	0.483
90.00-0	0.560
105.00-0	0.633
120.00-0	0.700
135.00-0	0.760
150.00-0	0.813
165.00-0	0.860
175.25-0	0.900
175.50-0	0.933
176.75-0	0.960
177.00-0	0.980
177.25-0	0.993
177.50-0	1.000
178.00-0	1.000
178.25-0	1.000
178.50-0	1.000
178.75-0	1.000
179.00-0	1.000
179.25-0	1.000
179.50-0	1.000
179.75-0	1.000
180.00-0	1.000

PASS 1 FOLLOWING

DELTTHETA=0.020 DEG,

TRJ	THETA	RHO	VT	DVDRH	DVDTH	RH-PR	RH-PPR	THD2	PHD2	PSI
STEP 0	2 170.92 0.896	0.	0.	2.475E+01	3.401E+03	5.344E+14	1.881E+17	2.428E-10		
3 170.92 1.000	0.	0.	1.789E+01	1.881E+03	1.092E+15	1.878E+17	9.77E-10			
4 179.73 3.000	0.	0.	1.334E+01	1.236E+03	1.715E+15	1.874E+17	2.182E-09			
5 179.54 1.050	0.	0.	1.362E+01	9.151E+02	2.310E+15	1.867E+17	3.071E-09			
6 179.55 1.000	0.	0.	8.921E+01	7.448E+02	2.787E+15	1.855E+17	6.325E-09			
7 179.56 1.000	0.	0.	7.538E+01	6.555E+02	3.031E+15	1.831E+17	8.625E-09			
8 179.57 1.000	0.	0.	6.576E+01	8.852E+02	1.981E+15	1.777E+17	1.154E-08			
STEP 1	5 170.92 0.8970 -5.829E-03	2.257E+03	0.	9.917E+00	2.274E+02	2.622E+15	5.156E+14	3.473E-10		
STEP 12	5 170.90 0.9594 -1.159E-02	2.363E+03	0.	9.466E+00	2.105E+02	2.652E+15	1.747E+13	9.595E-11		
STEP 18	5 170.28 0.9330 -1.730E-02	2.364E+03	0.	9.035E+00	1.958E+02	3.095E+15	2.664E+12	4.554E-11		
STEP 24	5 170.16 0.9220 -2.299E-02	2.507E+03	0.	8.638E+00	1.835E+02	3.251E+15	4.462E+11	2.784E-11		
STEP 31	5 170.04 0.9133 -2.854E-02	2.507E+03	0.	8.266E+00	1.713E+02	3.622E+15	1.385E+11	1.946E-11		
STEP 36	5 170.02 0.8964 -3.418E-02	2.651E+03	0.	7.917E+00	1.613E+02	3.907E+15	5.382E+10	1.479E-11		
STEP 42	5 170.00 0.8730 -3.944E-02	2.651E+03	0.	7.590E+00	1.509E+02	4.207E+15	1.452E+10	1.188E-11		
STEP 48	5 170.58 0.8564 -4.565E-02	2.923E+03	0.	7.283E+00	1.428E+02	4.522E+15	1.256E+10	9.922E-12		
STEP 54	5 170.56 0.8300 -5.053E-02	2.923E+03	0.	6.994E+00	1.339E+02	4.853E+15	7.637E+09	8.533E-12		
STEP 61	5 170.44 0.8255 -5.578E-02	2.923E+03	0.	6.672E+00	1.258E+02	5.202E+15	4.232E+09	7.544E-12		
177.25 0.	1.656E+01	2.228E+01	3.355E+01	4.555E+01	5.306E+01	4.476E+01	0.	0.	0.	0.
177.50 0.	1.575E+01	2.105E+01	2.979E+01	4.344E+01	7.322E+01	1.056E+02	1.244E+02	0.	0.	0.
177.75 0.	1.484E+01	1.976E+01	2.794E+01	4.066E+01	6.566E+01	8.738E+01	6.555E+01	0.	0.	0.
178.00 0.	1.375E+01	1.846E+01	2.654E+01	3.794E+01	6.022E+01	7.586E+01	7.454E+01	0.	0.	0.
178.25 0.	1.266E+01	1.707E+01	2.446E+01	3.533E+01	5.567E+01	9.976E+01	1.576E+02	2.20E+02	0.	0.
178.50 0.	1.125E+01	1.554E+01	2.206E+01	3.233E+01	5.13E+01	8.98E+01	1.82E+02	4.533E+02	0.	0.
178.75 0.	9.77E+00	1.355E+01	1.956E+01	2.922E+01	4.656E+01	8.14E+01	1.66E+02	2.84E+02	0.	0.
179.00 0.	8.16E+00	1.145E+01	1.676E+01	2.555E+01	4.13E+01	7.30E+01	1.44E+02	3.12E+02	3.24E+02	0.
179.25 0.	6.29E+00	8.93E+00	1.349E+01	2.036E+01	3.48E+01	6.266E+01	1.239E+02	2.633E+02	8.88E+02	0.
179.50 0.	4.19E+00	6.32E+00	9.24E+00	1.499E+01	2.57E+01	4.855E+01	9.59E+01	2.18E+02	5.1E+02	1.17E+03
179.75 0.	2.10E+00	3.61E+00	6.62E+00	7.53E+00	1.35E+01	2.71E+01	6.61E+01	1.43E+02	3.56E+02	8.47E+02
180.00 0.	0.	0.	0.	0.	0.	0.	0.	0.	0.	0.

DHS VALUES:
THI = 279.642 THF = 274.052

AXIAL POTENTIAL DISTRIBUTION

RHD	-V
0.632	0.261
0.700	0.397
0.760	0.413
0.813	0.395
0.846	0.331
0.900	0.269
0.933	0.220
0.960	0.177
0.980	0.127
0.992	0.067
1.000	0.

	INTEGRAL VALUES
1	0.001 (RAD)
2	0.0001
3	0.0001
4	0.0001
5	0.0001
6	0.0001
7	0.0001
8	0.001

**NO PAR **

POTENTIAL FIELD

POTENTIAL FIELD

```

OUTPUT-                                     RHC
THETA   0_20C  C_300  0_393  C_480  0_559  0_633  0_700  0_760  0_813  0_860  0_900  C_923  C_960  0_980  0_993  1_000
45. GC-1  G00C-1  C00U-1  -0.000-1  -0.000-1  -0.000-1  -0.000-1  -0.000-1  -0.000-1  -0.000-1  -0.000-1  -0.000-1  -0.000-1  -0.000-1  -0.000-1  -0.000-1
00. 00-0  B855-0  C_860-0  842L-0  0_828-0  8492-0  3_818-0  0_8055-0  0_8020-0  7999-0  0_7988-0  0_7984-0  7586-0  0_7989-0  0_7994-0  0_7998-0  0_8000-0
75. 00-0  7915-0  C_7456-0  7112-0  5_865-0  0_6636-0  0_6472-0  3_6345-0  0_6248-0  0_6174-0  0_6161-0  0_6077-0  0_6046-0  C_6048-0  0_6027-0  0_6131-0  0_6160-0  0_6194-0
90. 00-0  C_7414-0  6493-0  5997-0  0_5599-0  5_5271-0  4_9999-0  4774-0  C_4593-0  0_4437-0  0_4314-0  0_4216-0  0_4135-0  0_4082-0  0_4040-0  0_4044-0  0_4133-0  0_4199-0
105. 00-0  6498-0  0_5596-0  5057-0  4_5453-0  0_4949-0  3_3793-0  3_3352-0  3_0655-0  2_8101-0  0_7556-0  2_4017-0  2_273-0  2_124-0  2_080-0  2_0797-0  2_0262-0  0_2000-0
120. 00-0  5987-0  0_5168-0  4_342-0  0_3725-0  3_1328-0  2_2693-0  2_2247-0  1_839-0  0_1465-0  1_126-0  C_024-0  0_051-0  0_343-0  0_174-0  0_155-0  0_159-0
135. C-0  0_5601-0  4_62-0  3_846-0  0_3262-0  2_643-0  2_51-0  1_717-0  1_1338-0  1_013-0  0_0739-0  C_0514-0  3_34-0  C_1196-0  0_096-0  0_093-0  0_032-0
150. 00-0  5338-0  0_4379-0  3_3575-0  0_2969-0  2_459-0  2_131-0  1_1615-0  1_261-0  0_0954-0  0_694-0  C_0481-0  3_132-0  0_183-0  0_199-0  0_132-0  0_29-0
165. 00-0  5187-0  1_191-0  3_3501-0  0_3101-0  2_6679-0  0_24-0  3_2123-0  1_81-0  0_1455-0  1_193-0  0_07619-0  C_1502-0  0_295-0  0_145-0  0_148-0  0_148-0
176. 25-0  5242-0  4_156-0  3_517-0  0_3183-0  3_215-0  3_3750-0  4_191-0  C_4473-0  0_4346-0  0_3251-0  2_2220-0  0_1442-0  C_0845-0  0_448-0  0_438-0  0_438-0
176. 50-0  5141-0  4_156-0  3_517-0  0_3183-0  3_215-0  3_3750-0  4_242-0  0_4493-0  4_318-0  0_3309-0  0_2295-0  C_1546-0  0_4893-0  0_4444-0  0_446-0  0_446-0
176. 75-0  5242-0  4_156-0  3_517-0  0_3184-0  3_215-0  3_3768-0  4_6215-0  0_4504-0  4_3428-0  0_3367-0  0_2477-0  0_1571-0  0_1941-0  0_1471-0  0_1556-0
177. 00-0  5141-0  4_156-0  3_517-0  0_3185-0  3_2233-0  3_3775-0  4_6225-0  0_4513-0  0_4437-0  0_3416-0  0_2468-0  0_1444-0  0_3932-0  0_1502-0  0_1687-0
177. 25-0  5141-0  4_156-0  3_517-0  0_3186-0  3_2237-0  3_3781-0  4_6251-0  0_4534-0  0_4439-0  0_3549-0  0_2564-0  0_1724-0  0_1556-0  0_1538-0  0_179-0

```

177. 50-0. 51 45-0. 45 55-0. 35 17-0. 31 89-0. 32 30-0. 37 86-0. 42 42-0. 45 27-0. 43 49-0. 34 97-0. 26 42-0. 18 13-0. 11 14-0. 05 79-0. 04 194 U
 177. 75-0. 51 45-0. 45 55-0. 35 17-0. 31 88-0. 32 33-0. 37 71-0. 42 49-0. 45 32-0. 43 53-0. 35 28-0. 27 7-0. 19 12-0. 11 17-0. 05 29-0. 04 111 U
 178. 00-0. 51 35-0. 45 55-0. 35 17-0. 31 87-0. 32 36-0. 37 75-0. 42 53-0. 45 35-0. 35 54-0. 27 62-0. 22 6-0. 12 7-0. 05 89-0. 04 233 U
 178. 25-0. 51 35-0. 45 55-0. 35 18-0. 31 92-0. 32 39-0. 37 78-0. 42 58-0. 45 35-0. 35 56-0. 27 63-0. 22 8-0. 13 65-0. 05 765-0. 02 25 U
 178. 50-0. 51 35-0. 45 54-0. 35 17-0. 31 91-0. 32 41-0. 38 0-0. 42 65-0. 45 39-0. 34 55-0. 35 92-0. 28 46-0. 11 59-0. 04 178-0. 02 94 U
 178. 75-0. 51 35-0. 45 54-0. 35 18-0. 31 92-0. 32 42-0. 37 81-0. 42 62-0. 45 42-0. 34 55-0. 35 92-0. 28 46-0. 11 59-0. 04 178-0. 02 94 U
 179. 00-0. 51 35-0. 45 54-0. 35 18-0. 31 92-0. 32 44-0. 38 0-0. 42 63-0. 45 39-0. 34 54-0. 35 92-0. 28 46-0. 11 59-0. 04 178-0. 02 94 U
 179. 25-0. 51 35-0. 45 54-0. 35 18-0. 31 92-0. 32 45-0. 37 82-0. 42 64-0. 45 39-0. 34 55-0. 35 92-0. 28 46-0. 11 59-0. 04 178-0. 02 94 U
 179. 50-0. 51 35-0. 45 54-0. 35 18-0. 31 92-0. 32 46-0. 38 0-0. 42 65-0. 45 39-0. 34 56-0. 35 92-0. 28 46-0. 11 59-0. 04 178-0. 02 94 U
 179. 75-0. 51 35-0. 45 54-0. 35 18-0. 31 93-0. 32 46-0. 38 0-0. 42 65-0. 45 37-0. 34 48-0. 36 21-0. 25 20-0. 12 34-0. 04 184-0. 01 388-0. 01 688 U
 180. 00-0. 51 35-0. 45 54-0. 35 18-0. 31 93-0. 32 46-0. 38 0-0. 42 65-0. 45 37-0. 34 47-0. 36 24-0. 12 34-0. 04 184-0. 01 388-0. 01 688 U

TABLE OF RHC-VALUES FOR EQUIPOTENTIAL LINES

THETA	-0.90	-0.90	-0.70	-0.60	-0.50	-0.40	-0.30	-0.20	-0.10	
45.00	0.0	0.0	0.0	0.0	0.0	0.0	0.0	0.0	0.0	
60.00	0.175	0.050	0.0	0.0	0.0	0.0	0.0	0.0	0.0	
75.00	0.194	0.172	0.430	0.300	0.0	0.0	0.0	0.0	0.0	
90.00	0.170	0.149	0.222	0.393	0.633	1.000	0.0	0.0	0.0	
105.00	0.157	0.125	0.174	0.252	0.404	0.578	0.774	1.000	0.0	
120.00	0.050	0.100	0.149	0.199	0.309	0.441	0.587	0.726	0.877	
135.00	0.045	0.091	0.136	0.182	0.264	0.375	0.505	0.657	0.816	
150.00	0.043	0.086	0.129	0.172	0.233	0.341	0.476	0.625	0.805	
165.00	0.042	0.083	0.125	0.156	0.219	0.326	0.484	0.724	0.871	
176.25	0.041	0.082	0.123	0.165	0.214	0.327	0.487	0.659	0.953	
176.50	0.041	0.082	0.123	0.165	0.214	0.328	0.487	0.652	0.955	
176.75	0.041	0.082	0.123	0.165	0.214	0.329	0.487	0.646	0.957	
177.00	0.041	0.082	0.123	0.165	0.214	0.330	0.487	0.649	0.960	
177.25	0.041	0.082	0.123	0.165	0.214	0.331	0.488	0.652	0.962	
177.50	0.041	0.082	0.123	0.165	0.214	0.332	0.488	0.654	0.964	
177.75	0.041	0.082	0.123	0.165	0.214	0.333	0.488	0.656	0.967	
178.00	0.041	0.082	0.123	0.165	0.214	0.334	0.488	0.658	0.969	
178.25	0.041	0.082	0.123	0.165	0.214	0.335	0.489	0.660	0.972	
178.50	0.041	0.082	0.123	0.165	0.214	0.335	0.489	0.661	0.976	
178.75	0.041	0.082	0.123	0.165	0.214	0.335	0.489	0.664	0.983	
179.00	0.041	0.082	0.123	0.165	0.214	0.336	0.489	0.664	0.983	
179.25	0.041	0.082	0.123	0.165	0.214	0.336	0.489	0.665	0.985	
179.50	0.041	0.082	0.123	0.165	0.214	0.336	0.489	0.665	0.987	
179.75	0.041	0.082	0.123	0.165	0.214	0.336	0.489	0.665	0.987	
180.00	0.041	0.082	0.123	0.165	0.214	0.336	0.489	0.665	0.987	
STEP 0										
2	179.97	1.000	-3.80E-02	3.597E+04	0.0	2.075E01	5.410E03	5.118E+14	1.881E+17	2.428E+10
3	179.82	1.000	-3.93E-02	3.553E+04	0.0	1.789E01	2.883E+03	1.038E+15	1.872E+17	9.707E-10
4	179.73	1.000	-4.02E-02	3.516E+04	0.0	1.334E01	1.885E+03	1.617E+15	1.874E+17	2.182E-09
5	179.66	1.000	-3.95E-02	3.504E+04	0.0	1.052E01	1.410E+03	2.157E+15	1.867E+17	3.871E-09
6	179.55	1.000	-3.902E-02	3.491E+04	0.0	8.921E00	1.685E+03	2.563E+15	1.855E+17	6.029E-09
7	179.46	1.000	-3.869E-02	3.509E+04	0.0	7.538E00	1.606E+03	2.751E+15	1.831E+17	8.625E-09
8	179.37	1.000	-3.828E-02	3.569E+04	0.0	6.576E00	1.633E+03	1.655E+15	1.777E+17	1.154E-08
STEP 6										
2	179.79	0.050	-2.033E-01	1.516E+04	0.0	2.0172E01	1.637E+03	6.459E+14	7.115E+12	7.384E-12
3	179.70	0.566	-1.697E-01	1.818E+04	0.0	1.494E01	1.628E+02	1.233E+15	6.121E+12	4.554E-11
4	179.61	0.575	-1.500E-01	1.828E+04	0.0	1.024E01	5.257E+02	1.894E+15	2.505E+14	1.586E-10
5	179.52	0.580	-1.377E-01	1.837E+04	0.0	8.975E00	3.700E+02	2.486E+15	6.422E+14	3.885E-10
6	179.43	0.583	-1.279E-01	1.847E+04	0.0	7.458E00	5.313E+02	2.959E+15	1.213E+15	7.576E-10
7	179.34	0.586	-1.203E-01	1.864E+04	0.0	6.321E00	4.836E+02	3.210E+15	1.825E+15	1.254E-09
8	179.25	0.588	-1.127E-02	4.853E+04	0.0	4.893E00	6.908E+02	2.088E+15	2.341E+15	1.840E-09
STEP 12										
2	179.67	0.908	-2.797E-01	1.378E+04	0.0	1.0873E01	1.637E+03	7.745E+14	7.115E+12	7.384E-12
3	179.58	0.937	-2.289E-01	1.535E+04	0.0	1.337E01	6.835E+02	1.356E+15	1.785E+12	1.440E-11
4	179.49	0.952	-2.197E-01	1.547E+04	0.0	1.024E01	4.245E+02	2.042E+15	8.557E+12	4.753E-11
5	179.40	0.962	-2.173E-01	1.589E+04	0.0	8.241E00	3.337E+02	3.691E+15	2.707E+13	1.203E-10
6	179.31	0.968	-2.160E-01	1.918E+04	0.0	6.786E00	2.619E+02	3.617E+15	6.621E+13	2.523E-10
7	179.22	0.973	-2.145E-01	1.967E+04	0.0	5.602E00	2.619E+02	3.450E+15	1.335E+14	4.624E-10
8	179.13	0.979	-2.126E-01	2.042E+04	0.0	3.662E00	2.751E+02	2.271E+15	3.475E+14	9.382E-10
STEP 18										
2	179.55	0.871	-3.426E-01	1.405E+04	0.0	1.633E01	1.034E+03	9.126E+14	2.781E+16	1.787E-12
3	179.46	0.910	-2.743E-01	1.387E+04	0.0	1.209E01	5.642E+02	1.568E+15	2.301E+12	8.066E-12
4	179.37	0.932	-2.363E-01	1.395E+04	0.0	9.401E00	3.585E+02	2.277E+15	1.110E+12	2.524E-11
5	179.28	0.945	-2.093E-01	1.606E+04	0.0	7.627E00	2.758E+02	2.859E+15	3.696E+12	6.186E-11
6	179.19	0.955	-2.082E-01	1.643E+04	0.0	6.279E00	2.164E+02	3.387E+15	9.922E+12	1.308E-10
7	179.10	0.962	-2.095E-01	2.068E+04	0.0	5.150E00	1.010E+02	3.679E+15	2.298E+13	2.454E-10
8	179.01	0.967	-2.094E-01	2.144E+04	0.0	3.090E00	2.529E+02	2.530E+15	6.730E+13	6.009E-10
STEP 24										
2	179.43	0.839	-3.949E-01	1.252E+04	0.0	1.442E01	8.193E+02	1.061E+03	7.384E+06	1.371E-12
3	179.34	0.886	-3.162E-01	1.413E+04	0.0	1.098E01	4.944E+02	1.748E+03	5.646E+10	5.660E-12
4	179.25	0.913	-2.688E-01	1.405E+04	0.0	8.690E00	3.218E+02	2.475E+03	2.665E+11	1.684E-11
5	179.16	0.930	-2.380E-01	1.418E+04	0.0	7.081E00	2.337E+02	3.110E+03	8.993E+11	4.022E-11
6	179.07	0.942	-2.123E-01	1.700E+04	0.0	5.840E00	2.026E+02	3.603E+03	2.516E+12	8.460E-11
7	179.98	0.952	-2.189E-01	1.747E+04	0.0	4.769E00	1.714E+02	3.901E+03	6.302E+12	1.643E-10
8	178.89	0.966	-1.494E-01	2.294E+04	0.0	2.584E00	2.305E+02	2.914E+03	3.255E+12	4.559E-10
STEP 30										

SWITCH TO R-Z COORDINATE SYSTEM-

TRAJECTORY NO. 2 DELR=0.010

T+ETA	RHD	R	Z	DVDR	DVDZ	ZP	ZPP	V
123.32	0.090	0.075	-0.049	1.308E+00	-1.741E+00	1.255E+00	-5.165E+01	-8.156E-01
134.63	0.094	0.085	-0.039	1.333E+00	-1.687E+00	8.542E-01	-3.077E+01	-8.206E-01
108.56	0.100	0.095	-0.032	1.407E+00	-1.652E+00	6.072E-01	-1.974E+01	-6.183E-01
104.21	0.108	0.105	-0.027	1.308E+00	-1.614E+00	4.407E-01	-1.506E+01	-8.115E-01
101.25	0.117	0.115	-0.023	1.399E+00	-1.528E+00	3.109E-01	-1.202E+01	-8.028E-01
99.22	0.127	0.125	-0.020	1.414E+00	-1.471E+00	2.123E-01	-8.706E+00	-7.537E-01
97.93	0.136	0.135	-0.019	1.416E+00	-1.432E+00	1.343E-01	-7.001E+00	-7.821E-01
96.91	0.146	0.145	-0.019	1.419E+00	-1.407E+00	7.636E-02	-5.794E+00	-7.653E-01
96.31	0.156	0.155	-0.017	1.421E+00	-1.396E+00	1.735E-02	-4.905E+00	-7.557E-01
95.95	0.166	0.165	-0.017	1.422E+00	-1.381E+00	-2.819E-02	-4.23CE+00	-7.414E-01
95.77	0.176	0.175	-0.018	1.422E+00	-1.376E+00	-6.776E-02	-3.705E+00	-7.265E-01
95.72	0.186	0.185	-0.019	1.422E+00	-1.374E+00	-1.726E-01	-3.287E+00	-7.111E-01
95.77	0.196	0.195	-0.020	1.422E+00	-1.376E+00	-1.338E-01	-2.948E+00	-6.953E-01
95.90	0.206	0.205	-0.021	1.426E+00	-1.273E+00	-1.627E-01	-2.805E+00	-6.843E-01
96.10	0.216	0.215	-0.023	5.813E-01	-1.247E+00	-1.898E-01	-2.631E+00	-6.763E-01
96.34	0.227	0.225	-0.025	5.814E-01	-1.223E+00	-2.154E-01	-2.476E+00	-6.680E

97.26	C_257	0.255 -0.033	5.795E-11	-1.168E+00	-2.837E-01	-2.098E+00	-6.416E-01
97.52	C_268	0.265 -0.035	5.784E-01	-1.153E+00	-3.141E-01	-1.994E+00	-6.324E-01
97.99	C_278	0.275 -0.039	5.772E-01	-1.140E+00	-3.236E-01	-1.900E+00	-6.230E-01
98.26	C_288	0.285 -0.042	5.760E-01	-1.128E+00	-3.422E-01	-1.814E+00	-6.135E-01
98.75	C_299	0.295 -0.045	5.746E-01	-1.117E+00	-3.599E-01	-1.733E+00	-6.028E-01
99.15	C_305	0.305 -0.049	5.730E-01	-1.096E+00	-3.773E-01	-1.717E+00	-5.951E-01
99.54	C_320	0.315 -0.053	4.492E-01	-1.075E+00	-3.942E-01	-1.655E+00	-5.864E-01
99.94	C_330	0.325 -0.057	4.478E-01	-1.055E+00	-4.114E-01	-1.597E+00	-5.776E-01
100.35	C_341	0.335 -0.061	4.465E-01	-1.036E+00	-4.261E-01	-1.544E+00	-5.687E-01
100.75	C_351	0.345 -0.066	4.451E-01	-1.018E+00	-4.413E-01	-1.494E+00	-5.597E-01
101.15	C_362	0.355 -0.070	4.438E-01	-1.000E+00	-4.560E-01	-1.447E+00	-5.516E-01
101.55	C_373	0.365 -0.075	4.425E-01	-9.833E+00	-4.703E-01	-1.414E+00	-5.413E-01
101.95	C_383	0.375 -0.079	4.412E-01	-9.664E+00	-4.861E-01	-1.363E+00	-5.322E-01
102.35	C_394	0.385 -0.084	3.727F-01	-9.505E+00	-4.976E-01	-1.356E+00	-5.226E-01
102.74	C_405	0.395 -0.089	3.745E-01	-9.397E-01	-5.110E-01	-1.322E+00	-5.129E-01
103.14	C_416	0.406 -0.095	3.706E-01	-9.294E-01	-5.241E-01	-1.291E+00	-5.05CE-01
103.52	C_427	0.415 -0.100	3.693E-01	-9.189E-01	-5.368E-01	-1.261E+00	-4.960E-01
103.91	C_438	0.425 -0.105	3.682E-01	-9.084E-01	-5.493E-01	-1.233E+00	-4.876E-01
104.39	C_449	0.435 -0.111	3.671E-01	-8.980E-01	-5.615E-01	-1.206E+00	-4.778E-01
104.67	C_460	0.445 -0.117	3.660E-01	-8.767E-01	-5.734E-01	-1.181E+00	-4.666E-01
105.04	C_471	0.455 -0.122	4.142E-01	-7.900E-01	-5.846E-01	-8.342E-01	-4.594E-01
105.41	C_482	0.465 -0.128	3.724E-01	-7.678E-01	-5.929E-01	-8.362E-01	-4.507E-01
105.77	C_493	0.475 -0.134	3.715E-01	-7.574E-01	-6.011E-01	-8.211E-01	-4.424E-01
106.12	C_505	0.485 -0.140	3.706E-01	-7.472E-01	-6.093E-01	-8.067E-01	-4.344E-01
106.47	C_516	0.495 -0.146	3.697E-01	-7.371E-01	-6.173E-01	-7.929E-01	-4.255E-01
106.80	C_528	0.505 -0.153	3.688E-01	-7.271E-01	-6.251E-01	-7.797E-01	-4.176E-01
107.14	C_539	0.515 -0.159	3.680E-01	-7.172E-01	-6.329E-01	-7.676E-01	-4.085E-01
107.46	C_551	0.525 -0.165	3.671E-01	-7.075E-01	-6.445E-01	-7.548E-01	-3.999E-01
107.79	C_562	0.535 -0.172	3.661E-01	-6.972E-01	-6.560E-01	-7.548E-01	-3.913E-01
108.10	C_574	0.545 -0.178	3.648E-01	-6.878E-01	-6.555E-01	-7.457E-01	-3.829E-01
108.41	C_585	0.555 -0.185	3.640E-01	-6.763E-01	-6.529E-01	-7.370E-01	-3.745E-01
108.71	C_597	0.565 -0.191	3.631E-01	-6.654E-01	-6.702E-01	-7.286E-01	-3.666E-01
109.01	C_608	0.575 -0.198	3.638E-01	-6.550E-01	-6.775E-01	-7.204E-01	-3.575E-01
109.31	C_620	0.585 -0.205	3.635E-01	-6.458E-01	-6.847E-01	-7.125E-01	-3.485E-01
109.59	C_632	0.595 -0.212	3.367E-01	-6.366E-01	-6.917E-01	-7.048E-01	-3.412E-01
109.88	C_644	0.605 -0.219	3.220E-01	-6.239E-01	-6.988E-01	-7.057E-01	-3.317E-01
110.16	C_655	0.615 -0.226	3.211E-01	-6.164E-01	-7.058E-01	-7.058E-01	-3.231E-01
110.44	C_667	0.625 -0.233	3.201E-01	-6.588E-01	-7.129E-01	-6.962E-01	-3.145E-01
110.71	C_679	0.635 -0.240	3.192E-01	-7.122E-01	-7.198E-01	-6.915E-01	-3.057E-01
110.98	C_691	0.645 -0.247	3.182E-01	-7.335E-01	-7.267E-01	-6.870E-01	-2.976E-01
111.24	C_703	0.655 -0.255	3.119E-01	-7.743E-01	-7.335E-01	-6.856E-01	-2.882E-01
111.50	C_715	0.665 -0.262	3.107E-01	-7.785E-01	-7.404E-01	-6.840E-01	-2.793E-01
111.76	C_727	0.675 -0.269	3.096E-01	-7.827E-01	-7.472E-01	-6.824E-01	-2.714E-01
112.01	C_739	0.685 -0.277	3.084E-01	-7.868E-01	-7.540E-01	-6.807E-01	-2.614E-01
112.26	C_751	0.695 -0.285	3.073E-01	-7.908E-01	-7.618E-01	-6.790E-01	-2.524E-01
112.51	C_763	0.705 -0.292	3.076E-01	-7.960E-01	-7.676E-01	-6.775E-01	-2.432E-01
112.75	C_775	0.715 -0.300	3.061E-01	-8.021E-01	-7.744E-01	-6.787E-01	-2.34CE-01
112.99	C_788	0.725 -0.308	3.046E-01	-8.081E-01	-7.812E-01	-6.797E-01	-2.247E-01
113.23	C_800	0.735 -0.315	3.031E-01	-8.140E-01	-7.880E-01	-6.807E-01	-2.153E-01
113.46	C_812	0.745 -0.323	3.017E-01	-8.197E-01	-7.948E-01	-6.816E-01	-2.058E-01
113.69	C_825	0.755 -0.331	3.072E-01	-8.308E-01	-8.016E-01	-6.821E-01	-1.961E-01
113.92	C_837	0.765 -0.339	3.053E-01	-8.387E-01	-8.084E-01	-6.857E-01	-1.864E-01
114.15	C_850	0.775 -0.348	3.034E-01	-8.464E-01	-8.153E-01	-6.892E-01	-1.765E-01
114.37	C_862	0.785 -0.356	3.133E-01	-8.598E-01	-8.222E-01	-6.880E-01	-1.665E-01
114.60	C_875	0.795 -0.364	3.110E-01	-8.698E-01	-8.291E-01	-6.942E-01	-1.562E-01
114.82	C_887	0.805 -0.372	3.087E-01	-8.796E-01	-8.361E-01	-7.001E-01	-1.458E-01
115.04	C_900	0.815 -0.381	3.064E-01	-8.892E-01	-8.431E-01	-7.057E-01	-1.352E-01
115.25	C_912	0.825 -0.399	3.184E-01	-9.079E-01	-8.526E-01	-7.078E-01	-1.245E-01
115.47	C_925	0.835 -0.409	3.156E-01	-9.196E-01	-8.573E-01	-7.155E-01	-1.135E-01
115.68	C_938	0.845 -0.406	3.285E-01	-9.395E-01	-8.645E-01	-7.175E-01	-1.022E-01
115.89	C_951	0.855 -0.415	3.253E-01	-9.530E-01	-8.717E-01	-7.28CE-01	-9.085E-02
116.10	C_963	0.865 -0.424	3.370E-01	-9.742E-01	-8.790E-01	-7.320E-01	-7.915E-02
116.30	C_976	0.875 -0.433	3.334E-01	-9.892E-01	-8.864E-01	-7.437E-01	-6.714E-02
116.51	C_989	0.885 -0.441	3.419E-01	-1.011E+00	-8.938E-01	-7.505E-01	-5.482E-02
116.71	C_1002	0.895 -0.450	3.380E-01	-1.027E+00	-9.014E-01	-7.634E-01	-4.227E-02

APPENDIX B

FORTRAN PROGRAM

```
C*
C      PROGRAM FOR CALCULATING POTENTIAL FIELD IN AN AXISYMMETRIC
C      ELECTROSTATIC COLLECTOR. TAKING SPACE CHARGE INTO EFFECT.
C*
C      EXECUTIVE ROUTINE FOR PROCESSING MULTIPLE CASES
C      AND MAIN CONTROL OF LOGICAL FLOW THROUGHOUT PROGRAM.
C*
C***  
COMMON BO,CVF,DRHT(10),DRHM(16),DTHTD,DTHTR,DVDR(10),
1 DVDT(10),DVDR,DVRDZ,EQL(10),ETA0,IBAR,IT,JF,JP,KPO,KPOI,
2 KPOSC,LUOP,NEOL,N1,N2,N3,PHD2A(10),PI,PI2,PSIA(10),PSID(10),R,
3 RAD,RHM(17),RHOP(10),RHOPP(10),RHT(10),RHV(10),SPCH,TAU02,
4 THD(10),THMD(25),THSDEL,THSFAC,THSWHI,THSWLO,
5 THTD(10),THTR(10),TH1,TH2,V(17,25),VO,VR,
6 VSMT(10),VT(10),W(16),XCTR,XT(25,16),Y(16),ZJ0
    EQUIVALENCE (DTH,Y(1)),(TH,Y(2)),(RH,Y(3)),(RH2,RHP,Y(4)),
* (RH1P,Y(5)),(RH2P,Y(6)),(W(1),DELR),(W(2),ARI),
* (W(3),Z),(W(4),Z2,ZP),(W(5),Z1P),(W(6),Z2P)  
C***  
C      SUBROUTINES-
C      1. MAIN
C      2. INPUT
C      3. INTGRN
C      4. DE
C      5. DERIV
C      6. RK
C      7. MESH
C      8. RZTRAJ
C      9. RZRK(RZDE)
C     10. RZDE
C     11. OUT
C     12. VFIELD
C     13. EQLINS
C     14. RHSCAL(A,ZJ0,VO,TH1,THF,X,V2,IBAR,RHM,TH2)
C     15. PSICAL(R,Z,PSI,BO,ASM)
C     16. BRBZ (R,Z,BR,BZ,BO,ASM)  
C
10 FORMAT(5H0PASS,13.1X,8HFOLLOW-S)  
C
C      INITIALIZE SPACE CHARGE FIELD TO ZERO TO SET UP
C      LAPLACE EQUATION.
DO 1 I=1,16
DO 1 J=1,25
1 XT(J,I)=0.0  
C
C      INITIALIZE MESH SIZE, BOUNDARY CONDITIONS, CONVERGENCE
C      CRITERIA.
PI=0.0
LKTR=1
CALL INPUT
L=LOOP
```

```

C      COMPUTE POTENTIAL FIELD FOR GIVEN SPACE CHARGE FIELD.
2 CALL VFIELD
  IF(SPCH.EQ.0.) GO TO 3
C      CONDITIONAL OUTPUT OF POTENTIAL FIELD.
  WRITE(6,10) LKTR
3 CALL OUT
C      INTEGRATION OF ELECTRON CLASS TRAJECTORIES THROUGH
C      THE COMPUTED POTENTIAL FIELD.
  CALL INTGRN
  L=L-1
  LOOP=LOOP-1
  JT=1
  LKTR=LKTR+1
  CALL INPUT
  IF(L.GT.1) GO TO 2
C
  N1=2
  N2=8
  N3=1
  SPCH=0.0
  KPO=0
  IF(L.EQ.1) GO TO 2
C
  STOP
END

```

SUBROUTINE INPUT

```

C*
C*      READS AND PRINTS INITIAL CONDITIONS, PARAMETERS AND
C*      MISCELLANEOUS DATA REQUIRED FOR INTERNAL USE BY
C*      PROGRAM (OUTPUT FREQUENCY, LOOPING INDICES, CONVERGENCE
C*      CRITERIA, ETC.).
C*
C*** COMMON BO,CVF,DRHT(10),DRHM(16),DTHTD,DTHTR,DVDR(10),
1 DVDT(10),DVRDR,DVRDZ,EQL(10),ETA0,IBAR,IT,JF,JT,KPO,KPO1,
2 KPOSC,LOOP,NEQL,N1,N2,N3,PHD2A(10),PI,PI2,PSIA(10),PSI0(10),R,
3 RAD,RHM(17),RHOP(10),RHOPP(10),RHT(10),RHV(10),SPCH,TAUD2,
4 THD(10),THMD(25),THSDEL,THSFAC,THSWHI,THSWLO,
5 THTD(10),THTR(10),TH1,TH2,V(17,25),VO,VR,
6 VSM(10),VT(10),W(16),XCTR,XT(25,16),Y(16),ZJ0
    EQUIVALENCE (OTH,Y(1)),(TH,Y(2)),(RH,Y(3)),(RH2,RHP,Y(4)),
* (RH1P,Y(5)),(RH2P,Y(6)),(W(1),DELR),(W(2),AR),
* (W(3),Z),(W(4),Z2,ZP),(W(5),Z1P),(W(6),Z2P)
C*** 16 FORMAT(2X,3H10=,1PE13.3)
17 FORMAT(2X,3HJ0=,1PE13.3,4X,5HR =,E10.3)
18 FORMAT(2X,3HV0=,1PE13.3,4X,5HBU =,E10.3)
19 FORMAT(2X,6HCMFGA=,1PE10.3,4X,5HETA0=,E10.3)
20 FORMAT(2X,6FF0 =,1PE10.3,4X,5HKP =,E10.3)
21 FORMAT(1X,6HINPUT-)
22 FORMAT(40I2)
23 FORMAT(16H BRILLOUIN FLOW.)

```

```

24 FORMAT(/1X,12HOUTPUT EVERY.[2,1X,6HSTEPS.)
25 FORMAT(2X,6HTAU02=.E10.3,4X,5HRAD =,E10.3)
26 FORMAT(16F5.3)
27 FORMAT(3X,1HI,8X,4HDELI,9X,4HDELI,5X,5HTHETA,9X,3HVSM,
* 9X,2HVI,8X,6HINJEC.,8X,4HPSI0)
28 FORMAT(2X,12,2F13.3,F10.3,F12.3,1PE14.2,CPF10.3,1PE15.3)
29 FORMAT(16H0INITIAL VALUES-)
30 FORMAT(12X,5H(RADI),8X,5H(DEG),4X,5H(DEG),31X,6HANGLES)
31 FORMAT(1H1)
32 FORMAT(55H
33 FORMAT(8E10.3)
34 FORMAT(15H CONFINED FLOW.)
35 FORMAT(12,10F5.3)
36 FORMAT(/1X,29HCONE ANGLE IS OUT OF RANGE (=,F5.0,9H DEGREES))
37 FORMAT(/1X,30HSTEP SIZE TOO LARGE, DELTHETA=,F5.2)
38 FORMAT(/1X,32HCONFLICTING BOUNDARY CONDITIONS-)
39 FORMAT(2X,18HSURFACE POTENTIAL=.1PE9.2)
40 FORMAT(2X,15HBEAM POTENTIAL=.1PE9.2)
41 FORMAT(4F5.1)
42 FORMAT(24HNO SPACE CHARGE EFFECTS)
43 FORMAT(1X,12,21H ITERATIONS FOR SPACE)
44 FORMAT(15H CHARGE EFFECTS)

C
C
C      INITIALIZE TRAJECTORY CALCULATIONS.
C      FIRST TIME SETTING OF INITIAL CONDITIONS, BOUNDARY
C      PARAMETERS, CONVERGENCE CRITERIA.
JT=1
IF(PI.NE.0.) GO TO 9
C
C      CONSTANTS.
PI=3.14159265
PI2=2.*PI
CVF=180./PI
FO=8.860E-14
FTA0=1.753E+15
OM=1.414E+10
C
C      READ/WRITE.
WRITE(6,31)
READ(5,32)
WRITE(6,32)
READ(5,33) R,B0,DTHTD,TH1
READ(5,33) Z10,ZJ0,V0,DELR,CONFLO,RAD
READ(5,22) NT,KPO1,N1,N2,N3,IBAR,LOOP,KPOSC
C
C      INCREASE STEP SIZE DTH, BY A FACTOR
C      OF (THSFAC) EVERY (THSDEL) DEGREES
C      IN THE THETA(5) RANGE FROM (THSWHI)
C      TO (THSWL0) DEGREES.
READ(5,41) THSFAC,THSDEL,THSWHI,THSWL0
READ(5,26) IVSMI(I), I=1,NT
READ(5,35) NFOL, (EQL(I), I=1,NEQL)
TH2=177.-TH1/60.
JF=25
KPO=0
ZKP=710/(V0**1.5)
C

```

```

C      TEST MAGNITUDE OF CURRENT DENSITY
C      TO SEE IF SPACE CHARGE CALCULATIONS
C      SHOULD BE MADE.
SPCH=0.0
IF(ZJ0.LT.10.0) GO TO 14
SPCH=1.0
WRITE(6,43) LOOP
WRITE(6,44)
GO TO 15
14 WRITE(6,42)
15 TAU02=(R*R)/(2.*ETA0*VO)

C      INDICATE TYPE OF FLOW.
IF(CONFLD.F0.0.0) GO TO 1
WRITE(6,34)
GO TO 2
1 WRITE(6,23)
2 CONTINUE

C      READ BOUNDARY CONDITIONS.
READ(5,26) (XT(J,16), J=1,16)
DO 3 J=1,16
3 XT(J,16)=-XT(J,16)
XCTR=XT(1,16)
DO 4 I=1,15
4 XT(1,I)=XCTR

C      INPUT DATA CHECK.
IF(TH1.GE.0.0.AND.TH1.LE.174.) GO TO 5
WRITE(6,36) TH1
CALL EXIT
5 IF(DHTD.LT.0.0.AND.DHTD.GE.-.05) GO TO 6
WRITE(6,37) DHTD
CALL EXIT
6 IF(VSMI(1).LE.ABS(XCTR)) GO TO 7
TO=VSMI(NT)
WRITE(6,38)
WRITE(6,39) XCTR
WRITE(6,40) TO
CALL EXIT

C      INITIAL OUTPUT.
7 WRITE(6,21)
WRITE(6,20) EO,ZKP
WRITE(6,19) CM,ETA0
WRITE(6,16) ZIO
WRITE(6,17) ZJ0,R
WRITE(6,18) VO,BO
WRITE(6,25) TAU02,RAD
WRITE(6,24) KP0I
DHTR=DHTD/CVF

C      DETERMINE ENTRY CONDITIONS.
DIMENSION ALPH(10),DELI(10)
TO=RAD/FLOAT(NT-1)
DO 8 I=1,NT
T1=FI DAT(I-1)*TO
DELI(I)=ARSIN(T1/R)

```

```

ALPH(I)=1.0*FLOAT(I)
T2=PI-DELI(I)
ST=SIN(T2)
CT=COS(T2)
ARE=R*ST
ZED=R*(1.0+CT)
CALL PSICAL(ARE,ZED,PSI,B0,RAD)
PSIO(I)=PSI
IF(CONFLO.EQ.0.) PSIO(I)=0.0
8 CONTINUE
C
C      SETTING OF RHO-THETA VARIABLE MESH.
CALL MESH
C
C      SPREAD INITIAL TRAJECTORY VALUES.
C
C      EVERY TIME INITIALIZATION OF TRAJECTORIES.
9 DO 10 IT=2,NT
RHT(IT)=.9995
ALPHA=ALPH(IT)/CVF
GAMMA=PI-ALPHA-DELI(IT)+DTHTR
T2=-RHT(IT)/(DTHTR*SIN(GAMMA))
T3=SIN(ALPHA+DELI(IT))-SIN(GAMMA)
RH2P=-T2*T3
DRHT(I)=RH2P
RHOP(I)=RH2P
10 THD(IT)=VSMI(IT)/(1.+RHOP(IT)**2)
C
C      CALCULATE VT(I).
DO 11 I=1,NT
THTR(I)=PI-DELI(I)
THTD(I)=THTR(I)*CVF
11 VT(I)=V0*VSMI(I)
C
C      PRINT INITIAL TRAJECTORY VALUES.
WRITE(6,29)
WRITE(6,27)
WRITE(6,30)
DO 12 I=2,8
DELI0=DELI(I)*CVF
T1=180.-DELI0
12 WRITE(6,28)I,DELI(I),DELI0,T1,VSMI(I),VT(I),ALPH(I),PSIO(I)
C
DO 13 I=2,NT
IT=I
TH=THTR(IT)
RH=RHT(IT)
RHP=RHOP(IT)
CALL DE
13 RHOPP(IT)=RH2P
C
RETURN
END

```

SUBROUTINE INTGRN

```

C*
C*      CONTROLS INTEGRATION LOOPING OF EQUATIONS OF MOTION,
C*      STEP-SIZE, CHANGEOVER OF COORDINATE SYSTEMS AND THE
C*      NUMBER OF ITERATIONS REQUIRED FOR CONVERGENT SOLUTION.
C*
C*** COMMON BO,CVF,DRHT(10),DRHMI(16),DTHTD,DTHTR,DVDR(10),
1 DVDT(10),DVRDR,DVRDZ,EOL(10),ETA0,IBAR,IT,JF,JP,KPO,KPOI,
2 KPOSC,LOOP,NEOL,N1,N2,N3,PHD2A(10),PI,PI2,PSIA(10),PSID(10),R,
3 RAD,RHM(17),RHOP(10),RHOPP(10),RHT(10),RHV(10),SPCH,TAU02,
4 TH0(10),THMC(25),THSDEL,THSFAC,THSWHI,THSWLO,
5 THTD(10),THTR(10),TH1,TH2,V(17,25),VG,VR,
6 VSMI(10),VT(10),W(16),XCTR,XT(25,16),Y(16),ZJQ
EQUIVALENCE (DTH,Y(1)),(TH,Y(2)),(RH,Y(3)),(RH2,RHP,Y(4)),
* (RH1P,Y(5)),(RH2P,Y(6)),(W(1),DELR),(W(2),ARI),
* (W(3),ZI),(W(4),ZZ,ZP),(W(5),ZIP),(W(6),Z2P)
C*** 10 FORMAT(7H0DT+TD=.1PE9.2)
EXTERNAL DE
DTH=DTHTR
C
C      CHECK FOR SPACE CHARGE ITERATION.
IF(SPCH.EQ.0.) GO TO 1
N1=5
N2=5
N3=1
IF(LSW.EQ.9) GO TO 1
LSW=9
TH0=THTD(5)
C 1 DO 2 IT=N1,N2,N3
TH =THTR(IT)
RH =RHT(IT)
RHP=DRHT(IT)
RCLD=RH
CALL RK(DE)
RHOP (IT)=RHP
RHOPP(IT)=RH2P
THTR(IT)=TH
THTD(IT)=THTR(IT)*CVF
RHT(IT)=RH
2 DRHT(IT)=RHP
C
C      INCREASE STEP SIZE DTH, BY A FACTOR
C      OF (THSFAC) EVERY (THSDEL) DEGREES
C      IN THE THETA(5) RANGE FROM (THSWHI)
C      TO (THSWLO) DEGREES.
IF(THTD(5).GT.THSWHI) GO TO 3
IF(THTD(5).LE.THSWLO) THSWHI=0.0
THSWHI=THSWHI-THSDEL
DTH=THSFAC*DTH
T1=CVF*DTH
WRITE(6,10) T1
C 3 CONTINUE
JT=JT+1
CALL OUT
IF(SPCH.EQ.0.) GO TO 4
IF(RH.GT.RHM(7)) GO TO 1

```

```

THF=THTD(5)
CALL RHSCAL(RAD,ZJO,VO,THO,THF,XT,VSMI,IBAR,RHM,THMD(1),KPOS)
KPO=0
RETURN

C
C      R-Z COORDINATE TEST.
4 IF(THTR(2).GT.3.1) GO TO 5
IF(RHOP(N2).LT.0.) CALL RZTRAJ
5 IF(RHT(N1).GT.1.0) GO TO 6
GO TO 1

C
6 RETURN
END

```

SUBROUTINE DE

```

C*
C*      CONTAINS EQUATIONS OF MOTION IN SPHERICAL
C*      COORDINATE SYSTEM.
C*
C*** COMMON BO,CVF,DRHT(10),DRHM(16),DTHTD,DTHTR,DVDR(10),
1 DVDT(10),DVDR,DVRDZ,EOL(10),ETAO,IBAR,IT,JF,JT,KPO,KPOI,
2 KPOS.C,LOOP,NEQL,N1,N2,N3,PHD2A(10),PI,PI2,PSIA(10),PSIO(10),R,
3 RAD,RHM(17),RHOP(10),RHOPP(10),RHT(10),RHV(10),SPCH,TAUQ2,
4 THD(1G),THMD(25),THSDEL,THSFAC,THSWHI,THSWLO,
5 THTD(10),THTR(10),TH1,TH2,V(17,25),VO,VR,
6 VSMI(10),VT(10),W(16),XLTR,XT(25,16),Y(16),ZJO
EQUIVALENCE (DTH,Y(1)),(TH,Y(2)),(RH,Y(3)),(RH2,RHP,Y(4)),
* (RH1P,Y(5)),(RH2P,Y(6)),(W(1),DELR),(W(2),AR),
* (W(3),Z),(W(4),Z2,ZP),(W(5),Z1P),(W(6),Z2P)

C*** ST=SIN(TH)
ST2=ST**2
CT=COS(TH)

C      COMPUTE DV/DRHO AND DV/DTHETA.
CALL DERIV
ARE=RH*R*ST
ZED=R*(1.+RH*CT)

C      COMPUTE PSI.
CALL PSICAL(ARE,ZED,PSI,BO,RAD)

C      COMPUTE BR AND BZ.
CALL BRHZ(ARE,ZED,BR,BZ,BO,RAD)
T1=-FTAO/(ARE*ARE*PI2)
PHD=T1*(PSI-PSIO(IT))
PHD2=PHD**2
PHD2A(IT)=PHD2
PSIA(IT)=PSI

C      COMPUTES FIRST AND SECOND DERIVATIVES OF RHO WITH
C      RESPECT TO THETA (SPHERICAL COORDINATES).
DVMDRH=R*(BR*ST+BZ*CT)
DVMDTH=RH*R*(BR*CT-BZ*ST)
T1=RH*RH*R2*R*ST*PHD

```

```

PAR1=DVDR(IT)/R+ST*PHD*DVMDT
PAR2=DVOT(IT)/R-T1*DVMDRH
TO=(VSM((IT)+VT(IT))/(TAUG2*RH*RH*(1.+(RHP/RH)**2))
THD2=TO-(PHD2*ST2)/(1.+(RHP/RH)**2)
THD(IT)=THD2
T1=RH*ST*PHD
T2=(T1*ST*PHD)/THD2
T5=ETA0/R
T3=T5/THD2
T1=RH+T2+T3*PAR1
T2=-(RHP*ST*CT*PHD2)/THD2
T3=(2.*RHP**2)/RH
T4=-(RHP*T5)/(RH*RH*THD2)
RH2P=T1+T2+T3+T4*PAR2
RH1P=RH2
C
RETURN
END

```

SUBROUTINE DERIV

```

C*
C*      CALCULATES THE RATES OF CHANGE OF THE POTENTIAL
C*      FIELD IN SPHERICAL COORDINATES FOR ANY SPECIFIED
C*      INTERIOR POINT.
C*
C*** COMMON BO,CVF,DRHT(10),DRHM(16),DTHTD,DTHTR,DVDR(10),
1 DVOT(10),DVRDR,DVRDZ,EQL(10),ETAO,IBAK,IT,JF,JP,KPO,KPOI,
2 KPOSC,LOOP,NEQL,N1,N2,N3,PHD2A(10),PI,PI2,PSIA(10),PSIO(10),R,
3 RAD,RHM(17),RHOP(10),RHOPP(10),KHT(10),RHV(10),SPCH,TAU02,
4 THD(10),THMD(25),THSDEL,THSFAC,THSWHI,THSWLO,
5 THTD(10),THTR(10),TH1,TH2,V(17.25),VO,VR,
6 VSMI(10),YT(10),W(16),XCTR,XT(25.16),Y(16),ZJO
    EQUIVALENCE (OTH,Y(1)),(TH,Y(2)),(RH,Y(3)),(RH2,RHP,Y(4)),
* (RH1P,Y(5)),(RH2P,Y(6)),(W(1).DELRI),(W(2),AR),
* (W(3),Z1),(W(4),Z2,ZP),(W(5),Z1P),(W(6),Z2P)
C*** T2=TH*CVF
T3=15.
C
C      DETERMINE RHO INTERPOLATION FACTOR (FR).
DO 1 I=1,17
IF(RHM(I).GT.RH) GO TO 2
1 CONTINUE
2 IF(I.F0.17) I=16
FR=(RH-RHM(I-1))/DRHM(I-1)
C
C      DETERMINE THETA INTERPOLATION FACTOR (FT).
DO 3 J=1,25
IF(THMD(J).GT.T2) GO TO 4
3 CONTINUE
4 IF(T2.GT.TH2) T3=.25
FT=(T2-THMD(J-1))/T3
T3=T3/CVF
C
VP1=V(I-1,J-1)+FT*(V(I-1,J)-V(I-1,J-1))
VP2=V(I,J-1)+FT*(V(I,J)-V(I,J-1))

```

```

C VP3=V(I-1,J )+FR*(V(I ,J )-V(I-1,J ))
C VP4=V(I-1,J-1)+FR*(V(I ,J-1)-V(I-1,J-1))
C
C VT(IT)=VP1+FR*(VP2-VP1)
C     EVALUATES DV/DRHO AND DV/DTHETA AT (RH,T2) FROM CURRENT
C     POTENTIAL FIELD.
C DVDR(IT)=((VF2-VP1)/DRHM(I-1))*VG
C DVDT(IT)=((VF3-VP4)/T3)*VO
C IF(THTD(IT).GT.TH2) DVDT(IT)=0.0
C
C RETURN
C END

```

SUBROUTINE RK(DE)

```

C*
C     INTEGRATES ONE TRAJECTORY ONE STEP USING RUNGE-KUTTA
C     FORMULAS IN SPHERICAL COORDINATES.
C*
C*** COMMON BD,CVF,DRHT(10),DRHM(16),DTHTD,DTHTR,DVDR(10),
1 DVDT(10),DVDR,DVRDZ,EQL,IBAR,IT,JF,JP,KPO,KPOI,
2 KPOSC,LOOP,NEQL,N1,N2,N3,PHD2A(10),PI,PI2,PSIA(10),PSID(10),R,
3 RAD,RHM(17),RHOP(10),RHOPP(10),RHT(10),RHV(10),SPCH,TAUD2,
4 THD(10),THMC(25),THSDEL,THSFAC,THSWHI,THSWLO,
5 THTD(10),THTR(10),TH1,TH2,V(17,25),VO,VR,
6 VSMI(10),VT(10),W(16),XCTR,XT(25,16),Y(16),ZJ0
    EQUIVALENCE (DTH,Y(1)),(TH,Y(2)),(RH,Y(3)),(RH2,RHP,Y(4)),
* (RH1P,Y(5)),(RH2P,Y(6)),(W(1),DELR),(W(2),AR),
* (W(3),Z),(W(4),Z2,ZP),(W(5),Z1P),(W(6),Z2P)
C*** Y(15)=Y(3)
Y(16)=Y(4)
CALL DE
Y(7)=Y(1)*Y(5)
Y(8)=Y(1)*Y(6)
Y(2)=Y(2)+Y(1)/2.
Y(3)=Y(15)+.5*Y(7)
Y(4)=Y(16)+.5*Y(8)
CALL DE
Y(9)=Y(1)*Y(5)
Y(10)=Y(1)*Y(6)
Y(3)=Y(15)+.5*Y(9)
Y(4)=Y(16)+.5*Y(10)
CALL DE
Y(11)=Y(1)*Y(5)
Y(12)=Y(1)*Y(6)
Y(2)=Y(2)+Y(3)/2.
Y(3)=Y(15)+Y(11)
Y(4)=Y(16)+Y(12)
CALL DE
Y(13)=Y(1)*Y(5)
Y(14)=Y(1)*Y(6)
C
Y(3)=Y(15)+(Y(7)+2.*Y(9)+2.*Y(11)+Y(13))/6.
Y(4)=Y(16)+(Y(8)+2.*Y(10)+2.*Y(12)+Y(14))/6.

```

```
CALL DE
RETURN
END
```

SUBROUTINE MESH

```
C*
C*      FOR ANY SPECIFIED COLLECTOR GEOMETRY, GENERATES
C*      GRADUATED MESH POINT ARRAYS IN BOTH THE RHO AND
C*      THETA DIRECTIONS.
```

```
C***
```

```
COMMON BO,CVF,DRHT(10),DRHM(16),DTHTD,DTHTR,DVDR(10),
1 DVDT(10),DVRDR,DVRDZ,EUL(10),ETAO,IBAR,IT,JF,JT,KPO,KPOI,
2 KPOSC,LOOP,NEQL,N1,N2,N3,PHD2A(10),PI,PI2,PSIA(10),PSI0(10),R,
3 RAD,RHM(17),RHOP(10),RHOPP(10),RHT(10),RHV(10),SPCH,TAU02,
4 THD(10),THMD(25),THSDEL,THSFAC,THSWHI,THSWLO,
5 THT0(10),THTR(10),TH1,TH2,V(17,25),VO,VR,
6 VSMI(10),VT(10),W(16),XCTR,XT(25,16),Y(16),ZJC
EQUIVALNCE (DTF,Y(1)),(TH,Y(2)),(RH,Y(3)),(RH2,RHP,Y(4)),
* (RH1P,Y(5)),(RH2P,Y(6)),(W(1),DELR),,(W(2),AR),
* (W(3),Z),(W(4),Z2,ZP),(W(5),Z1P),(W(6),Z2P)
```

```
C***
```

```
C      GENERATE RHO AND DELRHO ARRAYS.
```

```
T1=0.8/120.
```

```
RHM(17)=1.0
```

```
C
```

```
C      GENERATE VARIABLE MESH RHO IN RHM ARRAY RANGING FROM
C      RHM(1)=0 TO RHM(17)=1 WITH FINE STEP AT END.
```

```
DO 1 I=1,16
```

```
J=17-I
```

```
DRHM(I)=FLOAT(I)*T1
```

```
1 RHM (J)=RHM(J+1)-DRHM(J)
```

```
DRHM(1)=0.2
```

```
RHM (1)=0.0
```

```
C
```

```
C      GENERATE THETA ARRAY.
```

```
JR=TH1/15.
```

```
JK=12-JR
```

```
C
```

```
C      GENERATE VARIABLE MESH THETA IN DEGREES IN THMD ARRAY
C      RANGING FROM THMD(1)=TH1 TO THMD(25)=180 WITH FINE STEP
C      AT END.
```

```
DO 2 J=1,JK
```

```
2 THMD(J)=TH1+.15.*FLOAT(J-1)
```

```
JK1=JK+1
```

```
JK2=JK+2
```

```
THMD(JK1)=177.-.25*FLOAT(JR)
```

```
TH2=THMD(JK1)
```

```
DO 3 J=JK2,JF
```

```
3 THMD(J)=THMD(JK1)+.25*FLOAT(J-JK1)
```

```
RETURN
```

```
FND
```

SUBROUTINE RZTRAJ

C*
C* CONTROLS INTEGRATION OF EQUATIONS OF MOTION IN THE
C* R-Z RECTILINEAR COORDINATE SYSTEM.
C* CONVERT FROM SPHERICAL COORDINATES (RHO,THETA) TO CYLINDRICAL
C* COORDINATES (R,Z) AND CONTINUE INTEGRATION OF TRAJECTORY UNTIL
C* IT REACHES SPHERICAL SURFACE.
C*
C***
COMMON BO,CVF,DRHT(10),DRHM(16),DTHTD,DTHTR,DVDR(10),
1 DVDT(10),DVDRDZ,DVRDZ,EUL(10),ETAO,IBAR,IT,JF,JT,KPO,KPOI,
2 KPOS,C,LOOP,NEQL,N1,N2,N3,PHD2A(10),PI,PI2,PSIA(10),PSIO(10),R,
3 RAD,RHM(17),RHOP(10),RHOPP(10),RHT(10),RHV(10),SPCH,TAUC2,
4 THD(10),THMD(25),THSDEL,THSFAC,THSWHI,THSWLO,
5 THTD(10),THTR(10),TH1,TH2,V(17,25),VO,VR,
6 VSMI(10),VT(10),W(16),XCTR,XT(25,16),Y(16),ZJ0
EQUIVALENCE (DTF,Y(1)),(TH,Y(2)),(RH,Y(3)),(RH2,RHP,Y(4)),
* (RH1P,Y(5)),(RH2P,Y(6)),(W(1),DELR),(W(2),ARI),
* (W(3),Z),(W(4),Z2,ZP),(W(5),Z1P),(W(6),Z2P)
C***
10 FORMAT(33H1SWITCH TO R-Z COORDINATE SYSTEM-)
11 FORMAT(15H TRAJECTORY NO.,I3,2X,5HDELR=,F4.3)
12 FORMAT(14X,5HTHETA,3X,3HRHO,5X,1HR,7X,1HZ,6X,4HDVDR,8X,4HDVDZ,9X,
* 2HZP,10X,3HZPP,10X,1HV)
13 FORMAT(2X,F7.2,3F7.3,1P5E12.3)
C
EXTERNAL RZDE
WRITE(6,10)
WRITE(6,11) N2,DELR
WRITE(6,12)
C
CONVERT TO R-Z COORDINATES.
AR=RHT(N2)*SIN(TH)
Z =RHT(N2)*COS(TH)
C
INITIALIZE R-Z INTEGRATION.
T0=RHOP(N2)*Z-RHT(N2)*AR
T1=RHT(N2)*Z+RHOP(N2)*AR
ZP=T0/T1
CALL RZDE
THRZ=90.-CVF*ATAN(Z/AR)
RHRZ=SQRT(AR*AR+Z*Z)
T2=DVRDZ-ZP*DVRDZ
T0=VSMI(IT)+VR
T1=1.+ZP**2
T3=2.* (T0/T1)
Z2P=T2/T3
WRITE(6,13) THRZ,RHRZ,AR,Z,DVDRDZ,ZP,Z2P,VR
C
INTEGRATE TO SURFACE.
1 CALL RZRK(RZDE)
THRZ=90.-CVF*ATAN(Z/AR)
RHRZ=SQRT(AR*AR+Z*Z)
WRITE(6,13) THRZ,RHRZ,AR,Z,DVDRDZ,ZP,Z2P,VR
IF(RHRZ.LT.1.0) GO TO 1
IF(N1.EQ.N2) T0=T0/0.0
C
N2=N2-1
RETURN
END

SUBROUTINE RZRK(RZDE)

C*

C INTEGRATES ONE TRAJECTORY ONE STEP USING RUNGE-KUTTA
C FORMULAS IN CYLINDRICAL COORDINATES.

C*

C***

```
COMMON BO,CVF,DRHT(10),DRHM(16),DTHTD,DTHTR,DVDR(10),
1 DVDT(10),DVRDR,DVRDZ,EQL(10),ETA0,IBAR,IT,JF,JT,KPO,KPOI,
2 KPOSC,LOOP,NEQL,N1,N2,N3,PHD2A(10),PI,PI2,PSIA(10),PSIO(10),R,
3 RAD,RHM(17),RHOP(10),RHOPP(10),RHT(10),RHV(10),SPCH,TAU02,
4 THD(10),THMC(25),THSDEL,THSFAC,THSWHI,THSWLG,
5 THTD(10),THTR(10),TH1,TH2,V(17,25),VO,VR,
6 VSMI(10),VT(10),W(16),XCTR,XT(25,16),Y(16),ZJC
EQUIVALENCE (DTH,Y(1)),(TH,Y(2)),(RH,Y(3)),(RH2,RHP,Y(4)),
* (RH1P,Y(5)),(RH2P,Y(6)),(W(1),DELR),(W(2),AR),
* (W(3),Z),(W(4),Z2,ZP),(W(5),Z1P),(W(6),Z2P)
```

C***

```
W(15)=W(3)
W(16)=W(4)
CALL RZDE
W(7)=W(1)*W(5)
W(8)=W(1)*W(6)
W(2)=W(2)+W(1)/2.
W(3)=W(15)+.5*W(7)
W(4)=W(16)+.5*W(8)
CALL RZDE
W(9)=W(1)*W(5)
W(10)=W(1)*W(6)
W(2)=W(15)+.5*W(9)
W(4)=W(16)+.5*W(10)
CALL RZDE
W(11)=W(1)*W(5)
W(12)=W(1)*W(6)
W(2)=W(2)+W(1)/2.
W(3)=W(15)+W(11)
W(4)=W(16)+W(12)
CALL RZDE
W(13)=W(1)*W(5)
W(14)=W(1)*W(6)
W(3)=W(15)+(W(7)+2.*W(9)+2.*W(11)+W(13))/6.
W(4)=W(16)+(W(8)+2.*W(10)+2.*W(12)+W(14))/6.
CALL RZDE
RETURN
END
```

SUBROUTINE RZDF

C COMPUTES FIRST AND SECOND DERIVATIVES OF Z WITH
C RESPECT TO R (CYLINDRICAL COORDINATES).

C*

C***

```
COMMON BO,CVF,DRHT(10),DRHM(16),DTHTD,DTHTR,DVDR(10),
1 DVDT(10),DVRDR,DVRDZ,EQL(10),ETA0,IBAR,IT,JF,JT,KPO,KPOI,
2 KPOSC,LOOP,NEQL,N1,N2,N3,PHD2A(10),PI,PI2,PSIA(10),PSIO(10),R,
3 RAD,RHM(17),RHOP(10),RHOPP(10),RHT(10),RHV(10),SPCH,TAU02,
```

```

4 THD(10),THMC(25),THSDEL,THSFAC,THSWHI,THSWLO,
5 THTD(10),THTR(10),TH1,TH2,V(17,25),VO,VR,
6 VSMI(10),VT(10),W(16),XCTR,XT(25,16),Y(16),ZJO
  EQUIVALENCE (DTF,Y(1)),(TH,Y(2)),(RH,Y(3)),(RH2,RHP,Y(4)),
* (RH1P,Y(5)),(RH2P,Y(6)),(W(1),DELR),(W(2),AR),
* (W(3),Z),(W(4),Z2,ZP),(W(5),Z1P),(W(6),Z2P)
C****
      RH=SORT(Z**2+AR**2)
      TH=ATAN2(AR,Z)
      CALL DERIV
      VR=VT(IT)
      DVRDR=(AR*DVER(IT)+(Z*DVRT(IT))/RH)/(RH*VO)
      DVRDZ=(Z*DVRD(IT)-AR*DVRT(IT)/RH)/(RH*VO)
      T1=DVRDZ-ZP*DVRDR
      T2=2.*((VSMI(IT)+VR)/(1.+ZP**2))
      Z2P=T1/T2
      Z1P=Z2
C
      RETURN
      END

```

SUBROUTINE OUT

```

C*
C       PRINTS OUT SELECTED DATA ALONG A TRAJECTORY.
C*
C****
COMMON BO,CVF,DRHT(10),DRHM(16),DTHTD,DTHTR,DVDR(10),
1 DVDT(10),DVRDR,DVRDZ,EOL(10),ETA0,IBAR,IT,JF,JT,KPO,KPOI,
2 KPOS2,LOOP,NEOL,N1,N2,N3,PHD2A(10),PI,PI2,PSIA(10),PSID(10),R,
3 RAD,RHM(17),RHOP(10),RHOPP(10),RHT(10),RHV(10),SPCH,TAUD2,
4 THD(10),THMC(25),THSDEL,THSFAC,THSWHI,THSWLO,
5 THTD(10),THTR(10),TH1,TH2,V(17,25),VO,VR,
6 VSMI(10),VT(10),W(16),XCTR,XT(25,16),Y(16),ZJO
  EQUIVALENCE (DTF,Y(1)),(TH,Y(2)),(RH,Y(3)),(RH2,RHP,Y(4)),
* (RH1P,Y(5)),(RH2P,Y(6)),(W(1),DELR),(W(2),AR),
* (W(3),Z),(W(4),Z2,ZP),(W(5),Z1P),(W(6),Z2P)
C****
C       FORMAT STATEMENTS.
10 FORMAT(10H0DELTHETA=,F7.4,5H DEG.)
11 FORMAT(5H STEP,15)
12 FORMAT(1X,3HTRJ,2X,5HTHETA,2X,3HRHO,6X,
     A 2HVT,7X,5HDVDRH,7X,5HDVDT,6X,5HRH-PR,6X,6HRH-PPR,6X,4HTHD2,
     B 6X,4HPHD2,6X,3HPSI)
13 FORMAT(1X,I2,F8.2,F6.3,1P8E11.3)
C
C       PRINT TITLES.
IF(K9.EQ.9) GO TO 1
K9=9
WRITE(6,10) DTHTD
WRITE(6,12)
C
1 IF(KPO.GT.1) GO TO 4
JT1=JT-1
WRITE(6,11) JT1
DO 2 I=N1,N2,N3

```

```
2 WRITE(6,13) I,THTD(I),RHT(I),VT(I),DVDR(I),
* DVDT(I),RFOP(I),RHOPP(I),THD(I),PHD2A(I),PSIA(I)
1 IF(RHT(N2).GT.1.0) GO TO 3
```

```
C
KPO=KPOI
RETURN
3 N2=N2-1
KPC=KPOI
RETURN
4 KPG=KPO-1
IF(RHT(N2).GE.1.0) GO TO 4
RETURN
END
```

SUBROUTINE VFIELD

```
C*
C
C      COMPUTES THE POTENTIAL FIELD V FOR A GIVEN SPACE CHARGE
C      FIELD BY SOLVING POISONS EQUATION.
C
C      POISS1 AND POISS2 ARE SUBROUTINES DESCRIBED BY THE TN
C      OF REFERENCE 2. THEY WERE DEVELOPED TO SOLVE POISONS
C      EQUATION IN A SUBREGION OF A SPHERE IN AN EFFICIENT
C      NON-ITERATIVE FASHION. USING A BLOCK DIAGONAL MATRIX
C      TECHNIQUE.
C*
COMMON/BLOCK1/NR,NT,RA(17),TA(25),X(25,16),X1,AVS
C***  
COMMON R0,CVF,DRHT(10),DRHM(16),DTHTD,DTHTR,DVDR(10),
1 DVDT(10),DVRDR,DVRDZ,EQL(10),ETA0,IBAR,IT,JF,JT,KPO,KPOI,
2 KPOSC,LOOP,NEQL,N1,N2,N3,PHD2A(10),PI,PI2,PSIA(10),PSID(10),R,
3 RAD,RHM(17),RHOP(10),RHOPP(10),RHT(10),RHV(10),SPCH,TAU02,
4 THD(10),THMD(25),THSDEL,THSFAC,THSWHI,THSWLO,
5 THTD(10),THTR(10),TH1,TH2,V(17,25),VO,VR,
6 VSMI(10),VT(10),W(16),XCTR,XT(25,16),Y(16),ZJ0
    EQUIVALENCE (DTF,Y(1)),(TH,Y(2)),(RH,Y(3)),(RH2,RHP,Y(4)),
* (RH1P,Y(5)),(RH2P,Y(6)),(W(1),DELR),(W(2),AR),
* (W(3),Z),(W(4),ZZ,ZP),(W(5),Z1P),(W(6),Z2P)
C***  
LOGICAL AVS
DIMENSION XB(15),TD(25)
C
23 FORMAT(16F5.3)
24 FORMAT(1X,F6.2,1P12E10.2)
25 FORMAT(7H INPUT-,52X,3HRHO)
26 FORMAT(11H0**NO BAR**)
27 FORMAT(13H0 EAR VALUES-)
28 FORMAT(4X,1HR,8X,1HV)
29 FORMAT(2X,F5.3,3X,F6.3)
30 FORMAT(8H OUTPUT-,52X,3HRHO)
31 FORMAT(6H THETA,3X,16(F5.3,2X))
32 FORMAT(6H THETA,3X,12(F5.3,5X))
33 FORMAT(4H X1=,F5.2)
34 FORMAT(1X,F6.2,16F7.4)
35 FORMAT(15H POTENTIAL FIELD)
```

```

C
X1=XCTR
NR=17
NR1=NR-1
NR2=NR-2
DO 1 I=1,17
1 RA(I)=RHM(I)
NT=JF
NT1=NT-1
DO 2 J=1,NT
DO 2 K=1,NR1
2 X(J,K)=XT(J,K)

C
C           IF AXIAL SPIKE IS PRESENT IN THIS PARTICULAR PROBLEM,
C           READ IN THESE VALUES AND DISPLAY THEM. -
IF(IBAR.EQ.0) GO TO 4
DO 3 I=1,NR2
3 X(NT,I)=XB(I)
4 DO 5 J=1,NT
TC(J)=THMD(J)
5 TA(J)=THMD(J)/CVF
IF(IBAR.EQ.0) GO TO 9

C
C           READ BAR VALUES.
AVS=.TRUE.
IF(LSW.EQ.9) GO TO 7
LSW=9
READ(5,23) (X(NT,I), I=1,NR1)
DO 6 I=1,NR2
XB(I)=-X(NT,I)
6 X(NT,I)=-X(NT,I)

C
C           PRINT BAR VALUES.
7 WRITE(6,27)
WRITE(6,28)
WRITE(6,29) RA(1),X1
DO 8 I=1,NR1
J=I+1
8 WRITE(6,29) RA(J),X(NT,I)
GO TO 10
9 AVS=.FALSE.
WRITE(6,26)

C
C           SET-UP AND FACTOR SUB-MATRICES IN BLOCK DIAGONAL
C           COEFFICIENT MATRIX.
10 CALL POISS1

C
C           PRINT INPUT BLOCK.
WRITE(6,35)
WRITE(6,25)
WRITE(6,32) (RA(I), I=6,NR)
DO 11 J=1,NT
11 WRITE(6,24) TD(J), (X(J,K-1), K=6,NR)
WRITE(6,33) X1

C
C           CARRY OUT SOLUTION OF MATRIX PROBLEM TO YIELD V-FIELD.
CALL POISS2

```

```

C      ADJUST BAR VALUES.
IF(LBAR.EQ.0) GO TO 17
DO 16 I=4,16
16 X(NT,I)=X(NT1,I)
C
C      PRINT OUTPUT BLOCK.
17 WRITE(6,35)
  WRITE(6,30)
  WRITE(6,31) (RA(I), I=2,NR)
  DO 12 J=1,JF
12 WRITE(6,34) TD(J),(X(J,K-1),K=2,NR)
  DO 13 J=2,JF
  DO 13 K=1,15
13 XT(J,K)=X(J,K)
C
C      DISPLAY EQUIPOTENTIAL LINE DATA.
IF(LOOP.LE.1) CALL EQLINE
  DO 14 J=1,JF
14 V(I,J)=XCTR
  DO 15 I=2,17
  K=I-1
  DO 15 J=1,JF
15 V(I,J)=XT(J,K)
C
      RETURN
      END

```

SUBROUTINE ECLINE

```

C*
C
C      FIND ON EACH THETA MESH LINE THE RHO VALUES ASSOCIATED
C      WITH NEQL PRE-SPECIFIED POTENTIAL VALUES. AN EQUIPOTENTIAL
C      CURVE PASSES THROUGH SETS OF THESE POINTS.
C*
C*** COMMON BO,CVF,DRHT(1G),DRHM(16),DTHTD,UTHTR,DVDR(10),
1 DVDT(10),DVRDR,DVRDZ,EWL(10),ETAO,LBAR,IT,JF,JT,KPC,KPOI,
2 KPOSC,LOOP,NEQL,N1,N2,N3,PHD2A(10),PI,PI2,PSIA(10),PSIO(10),R,
3 RAD,RHM(17),RHOP(10),RHUPP(10),RHT(10),RHV(10),SPCH,TAU02,
4 THD(10),THMD(25),THSDEL,THSFAC,THSWHI,THSWLO,
5 THTD(10),THTR(10),TH1,TH2,V(17,25),VO,VR,
6 VSMI(10),VT(10),W(16),XCTR,XT(25,16),Y(16),ZJ0
  EQUIVALENCE (DT,Y(1)),(TH,Y(2)),(RH,Y(3)),(RH2,RHP,Y(4)),
* (RH1P,Y(5)),(RH2P,Y(6)),(W(1),DELR),(W(2),AR),
* (W(3),Z1),(W(4),Z2,ZP),(W(5),Z1P),(W(6),Z2P)
C*** 10 FORMAT(/28X,23HTABLE OF RHO-VALUES FOR)
11 FORMAT(30X,1SH EQUIPOTENTIAL LINES)
12 FORMAT(1X,F6.2,2X,10F10.3)
13 FORMAT(2X,5HTHETA.2X,10(F10.2))
C
C      ZERO OUT RHV-ARRAY.
  DO 6 I=1,10
6 RHV(I)=0.0
C
  WRITE(6,10)
  WRITE(6,11)

```

```

NR=17
WRITE(6,13) (EQL(I), I=1,NEQL)
C
DO 5 J=1,JF
DO 4 I=1,NEQL
DO 1 K1=1,NR
K=NR-K1
IF(EQL(I).GT.XT(J,K)) GO TO 2
1 CONTINUE
C
2 IF(K1.GT.1) GO TO 3
RHV(I)=0.0
GO TO 5
C
3 F=(XT(J,K)-EQL(I))/(XT(J,K)-XT(J,K+1))
IF(K.GT.0) GO TO 4
F=(XCTR-EQL(I))/(XCTR-XT(J,K+1))
4 RHV(I)=RHM(K+1)+F*(RHM(K+2)-RHM(K+1))
5 WRITE(6,12) THMD(J), (RHV(I), I=1,NEQL)
C
RETURN
END

```

```

SUBROUTINE RHSCAL(A,ZJO,V0,TH0,THF,X,V2,IBAR,RHM,TH2,KPOS)
C*
C      RIGHT-HAND SIDE CALCULATION FOR POISSON MATRIX EQUATION.
C      EQUIVALENT TO CALCULATION OF SPACE CHARGE FIELD.
C*
DIMENSION V(11),C(9),VI(10),RH(11),AD(11),RHS(11,9),ARG(16),
*           TH(11,9),THR(11,9),RHSI(10,16),X(25,16),V2(10),RHM(17)
C
C      FORMAT STATEMENTS.
22 FORMAT(1X,F5.3,F7.3)
23 FORMAT(16F5.0)
24 FORMAT(11HORHS ARRAY-)
25 FORMAT(1X,16F8.1)
26 FORMAT(2X,16F8.2)
27 FORMAT(10F5.0)
28 FORMAT(/2X,3HRHO,5X,2H-V)
29 FORMAT(12HORHS VALUES.)
30 FORMAT(/2X,3HRHO,4X,1HC,2X,4HTUBE,4X,5HTHETA,6X,3HRHS)
31 FORMAT(1X,F5.3,2I4,1H-,I1,F10.3,F9.1)
32 FORMAT(5H TH1=,F7.3,7X,5HTHF =,F8.3)
33 FORMAT(/4X,5FAXIAL/2X,9HPOTENTIAL/1X,12HDISTRIBUTION)
C
C      A=RADIUS OF ENTRY HOLE.
C      ZJO=JO (CURRENT DENSITY).
C      TH0=INITIAL VALUE OF TRAJECTORY 5.
C      X=XT(25,16), SOURCE TERMS.
C      V2=ENERGY CLASSES.
C      TH2=CONF ANGLE.
TH1=TH0
IF=11
JF= 7
JF1=JF+1
JF2=JF+2
ENT=8.

```

```

E0 = 8.860E-14
ETA=1.753E+15
C1 =2.*E0*SQRT(2.*ETA)*ENT*ENT
PI =3.14159265
CVF=180./PI
WRITE(6,29)
WRITE(6,32) TH0,THF
C
C SECTION FOR COMPUTING SPACE CHARGE ALONG
C TUBE CENTER LINES.
C I=BIG LOOP FOR 11 RHO VALUES FROM 0.63 TO 1.00
C J=SM. LOOP FOR 7 TUBES (1-2,2-3,...,7-8).
C THF=RHO .63 CROSSING ANGLE OF TRAJ. NO. 5.
C READ 11 AXIAL V-VALUES(RHO .63 TO 1.0)
C AND VSMI-ARRAY(9).
C
C GENERATE ARG-ARRAY, C-ARRAY, AND VI-ARRAY.
C ARG(K)=THETA MESH VALUES IN HOLE REGION.
C C (J)=1,3,5,...,13 (MULTIPLIERS).
C VI (J)=1.55,1.40,...,0.4,0.0 (ENERGY CLASSES IN TUBES).
C
DO 1 K=1,16
1 ARG(K)=180.-FLOAT(K)*.25
DO 2 J=1,JF
VI(J)=(V2(J)+V2(J+1))/2.
2 C(J)=2*J-1
C
C GENERATE AND PRINT RH-ARRAY AND V-ARRAY.
C RH(I) ARRAY-11 AXIAL RHO MESH VALUES
C FROM .633 TO 1.000
C V (I)-POTENTIAL DISTRIBUTION AT THESE
C 11 AXIAL MESH POINTS.
C
WRITE(6,33)
WRITE(6,28)
DO 3 I=1,IF
RH(I)=RHM(I+6)
V(I)=-X(25,I+5)
3 WRITE(6,22) RH(I),V(I)
C
C GENERATE THETA-ARRAY AND SPREAD THROUGHOUT
C SPACE CHARGE REGION (BASED ON TRAJECTORY NO. 5).
C
DTH=TH1-THF
ORD=1.-RHM(7)
TO=DTH/ORD
DO 5 I=1,IF
I6=I+6
DIFF=RHM(I6)-RHM(7)
T1=THF+TO*DIFF
T2=T1+(180.-T1)/8.
DEL=(180.-T2)/4.
DO 4 J=1,JF2
THD(I,J)=180.-FLOAT(J)*DEL
4 THR(I,J)=THD(I,J)/CVF
5 CONTINUE
C
C GENERATE AD-ARRAY (DISTANCE BETWEEN
C TRAJECTORIES 4 AND 5 AT EACH OF
C 11 RHO MESH LINES).
C
DO 6 I=1,IF
TX1=RH(I)*TAN(THR(I,5))
TX2=RH(I)*TAN(THR(I,4))

```

```

6 AD(I)=TX2-TX1
C
C      CALCULATE SOURCE TERMS FOR ALL TRAJECTORY
C      CROSSINGS OF RHO MESH LINES.
AJ=A*A*ZJ0
DO 9 I=1,IF
  IF(KP0SC.NE.0) WRITE(6,30)
DO 9 J=1,JP
  E1=VI(J)-V(I)
  IF(E1.GT.0.) GO TO 7
  RHS(I,J)=0.0
  GO TO 8
7 F2=SQRT(E1)
  ST=SIN(THR(I,J))
  DEN=C1*SORT(V0**3)*E2*RH(I)*ST*AD(I)
  RHS(I,J)=(C(J)*AJ)/DEN
8 J1=J+1
  IC=C(J)
  IF(KP0SC.NE.0) WRITE(6,31) RH(I),IC,J,J1,THD(I,J),RHS(I,J)
9 CONTINUE
C
C      SECTION FOR INTERPOLATING SPACE CHARGE FIELD AT MESH POINTS.
DO 15 I=1,10
DO 15 K=1,16
DO 10 J=1,7
  IF(ARG(K).GT.THD(I,J)) GO TO 11
10 CONTINUE
11 IF(J.NE.1) GO TO 13
  DELRHS=0.-RHS(I,J)
  T1=180.-THD(I,J)
12 T2=ARG(K)-THD(I,J)
  F=T2/T1
  IF(ARG(K).LT.THD(I,J)) GO TO 14
    T1=RHS(I,J)+F*DELRHS
  RHS(I,K)=(RHS(I,K)+T1)/2.
  GO TO 15
13 T1=THD(I,J-1)-THD(I,J)
  DFLRHS=RHS(I,J-1)-RHS(I,J)
  GO TO 12
14 RHS(I,K)=0.0
15 CONTINUE
  IF(KP0SC.EQ.0) GO TO 17
C
C      PRINT.
  WRITE(6,24)
  WRITE(6,26) (ARG(K), K=1,16)
  DO 16 I=1,10
16 WRITE(6,25) (RHS(I,K), K=1,16)
C
C      ZERO OUT RHS PREPARATORY TO
C      LOADING SOURCE TERMS.
17 DO 18 J=2,24
  DO 18 K=1,15
18 X(J,K)=0.0
  IF(TBAR.NE.0) GO TO 20
  DO 19 I=1,16
19 X(25,I)=0.0

```

```
C
20 J2=13.-TH2/15.
00 21 J=J2,24
00 21 K=6,15
J1=25-J
K1=K-5
21 X(J,K)=RHSI(K1,J1)
```

```
C
RETURN
END
```

SUBROUTINE PSICAL(R,Z,PSI,B0,ASM)

```
C*
C*      CALCULATES PSI, THE MAGNETIC FLUX, OF THE MAGNETIC
C*      FIELD AT EACH MESH POINT IN THE REGION OF THE
C*      ENTRY HOLE.
```

```
C*
PI=3.14159265
RF=R
RSQ=R*R
X= Z/ASM
X2 = X*X
AT = ATAN2(ASM,-Z)
```

```
C
T= 1.+X2
T0 = PI-AT-X/T
T4 = 3.-5.*X2
T6= 3.-7.*X2*(2.-X2)
T= 21.-5.*X2
T= 15.-X2*T
T8= 5.-3.*X2*T
T= 36.-5.*X2
T= 54.-X2*T
T= 20.-X2*T
T10=9.*(15.-11.*X2*T)
T= 11.-X2
T= 7.*X2*T
T= 198.-T
T= 154.-X2*T
T= 35.-X2*T
T12 = 21.-13.*X2*T
```

```
C
X1= ASM*(1.+X2)
V= (RF/X1)**2
```

```
C
T= (21.*T10)/5.+(11.*T12*V)/4.
T= 7.*T8+0.5*V*T
T=(5.*T6)/3.+125*V*T
T= T4/4.+125*V*T
T= 1.+V*T
T= T0-(ASM*X*RSQ*T)/(X1**3)
PSI= B0*RSQ*T
```

```
C
RETURN
END
```

SUBROUTINE BFBZ(R,Z,BR,BZ,B0,ASM)

```

C*
C*      CALCULATES BR AND BZ, THE R AND Z COMPONENTS OF THE
C*      MAGNETIC FIELD AT EACH MESH POINT IN THE REGION
C*      OF THE ENTRY HOLE.
C*
C*      PI=3.14159265
C*      IF(Z.EQ.0.0) Z=.0004
C*      X=Z/ASM
C*      X2=X**2
C
C      T1=1.
C      T2=1.
C      T3=1.-5.*X2
C      T4=3.-5.*X2
C      T5=3.-7.*X2*(6.-5.*X2)
C      T6=3.-7.*X2*(2.-X2)
C      T7=1.-X2*(27.-7.*X2*(9.-3.*X2))
C      T8=5.-3.*X2*(15.-X2*(21.-5.*X2))
C      T9=30.-X2*(28.-5.*X2)
C      T9=5.-11.*X2*(20.-3.*X2*T9)
C      T10=54.-X2*(36.-5.*X2)
C      T10=20.-X2*T10
C      T10=9.*(15.-11.*T10*X2)
C
C      T11=18.-X2*(9.-X2)
C      T11=195.-143.*X2*(10.-X2*T11)
C      T11=3.-X2*T11
C      T12=-X2*(1001.-91.*X2)
C      T12=-X2*(2574.+T12)
C      T12=-X2*(2002.+T12)
C      T12=-X2*( 455.+T12)
C      T12=11.*(21.+T12)
C      T1B=(ASM*Z)/(ASM*ASM+Z*Z)
C
C      ZK=1.+X2
C      A1=ASM*ZK
C      A2=ASM*ZK*X
C
C      C1=(-2.*B0)/(PI*ASM*ZK*ZK)
C      C2=(-4.*C1*X)/A1
C      C3=C2/A2
C      C4=(-6.*C3*X)/A1
C      C5=C4/A2
C      C6=(-40.*C5*X)/A1
C      C7=(3.*C6)/A2
C      C8=(-14.*C7*X)/A1
C      C9=C8/A2
C      C10=(-4.*C9*X)/A1
C      C11=(45.*C10)/A2
C      C12=(-2.*C11*X)/A1
C
C      AT=ATAN2(ASM,-Z)
C      BB=(B0/PI)*(PI-AT-T1B)
C      B 1=C 1*T 1
C      B 2=C 2*T 2
C      B 3=C 3*T 3
C      B 4=C 4*T 4
C      B 5=C 5*T 5
C      B 6=C 6*T 6

```

B 7=C 7*T 7
B 8=C 8*T 8
B 9=C 9*T 9
B10=C10*T10
B11=C11*T11
B12=C12*T12

C

R2=R/2.
RS=R2*R2
T1=B10-RS*B12/36.
T1=BB-RS*T1/25.
T1=B6-RS*T1/16.
T1=B4-RS*T1/5.
T1=B2-RS*T1/4.
BZ=BB-RS*T1

C

T1=B9-B11*RS/30.
T1=B7-RS*T1/20.
T1=B5-RS*T1/12.
T1=B3-RS*T1/6.
T1=B1-RS*T1/2.
BR=-R2*T1

C

RETURN
END

APPENDIX C

FORTRAN SYMBOLS

ALPH(10)	array of entry angles, α , rad
ALPHA	entry angle, α , deg
AR	rectilinear coordinate, r
ASM	radius of entry hole, a, cm
AVS	axial boundary value logical switch TRUE indicates presence of an axial spike
B0	magnetic flux density, B_0
BR	r-component of magnetic field, B_r
BZ	z-component of magnetic field, B_z
CONFLO	switch for type of flow (confined flow when not equal to 0; Brillouin flow when equal to 0)
CVF	conversion factor, deg to rad
DELI(10)	δ_i array, rad
DELID	entry angles of electron classes, δ_i , deg
DELR	step size Δr for r-z trajectory integration
DRHM(16)	$\Delta\rho$ of mesh
DRHT(10)	$\Delta\rho$ of trajectories
DTH	$\Delta\theta$ of trajectories (equivalent to DTHTR below), rad
DTHTD	$\Delta\theta$ of trajectories (step in θ for $\rho-\theta$ trajectory integration), deg
DTHTR	$\Delta\theta$ of trajectories, rad
DVDR(10)	$\partial V/\partial \rho$ array
DVDT(10)	$\partial V/\partial \theta$ array
DVMDRH	$\partial V_m/\partial \rho$ array
DVMDTH	$\partial V_m/\partial \theta$
DVRDR	$\partial V_r/\partial r$
DVRDZ	$\partial V_r/\partial z$
EQL(10)	array of values for which equipotential lines are to be calculated

ETA0	initial electron charge-to-mass ratio
E0	permittivity of free space, ϵ_0
FLOOP	storage for number of iteration loops in space charge calculation
IBAR	indicator for axial boundary values
IT	iteration counter
J1, J2, JF, JT	looping indexes
KPO, KPOI	main output frequency control of trajectory data (e.g., 5 means to print every fifth point); KPOI is constant; KPO may be varied
KPOSC	output control for space charge values
K9	initialization switch
LKTR	counter for number of loops
LOOP	indicator switch for space charge looping
NEQL	number of equipotential lines to be calculated
N1, N2, N3	control indexes for trajectory calculations
NF	number of θ -mesh lines, usually 26
NR	number of ρ -mesh points, usually 17
NT	number of trajectories, usually 9
PHD	$\dot{\varphi}(\partial\varphi/\partial t)$, where φ is azimuthal angle
PHD2	$\dot{\varphi}^2$
PHD2A(10)	$\dot{\varphi}^2$ array for output
PI, PI2	π, π^2
PSI	magnetic flux, ψ
PSIA(10)	ψ array
PSI0	initial magnetic flux, ψ_0
R	radius of collector, R, cm
RA(17)	array of r-mesh values
RAD	radius of entry hole, a, cm
RH, RHP	$\rho, \rho'(\partial\rho/\partial\theta)$
RH1P	ρ'_1
RH2, RH2P	ρ'_2, ρ'_2

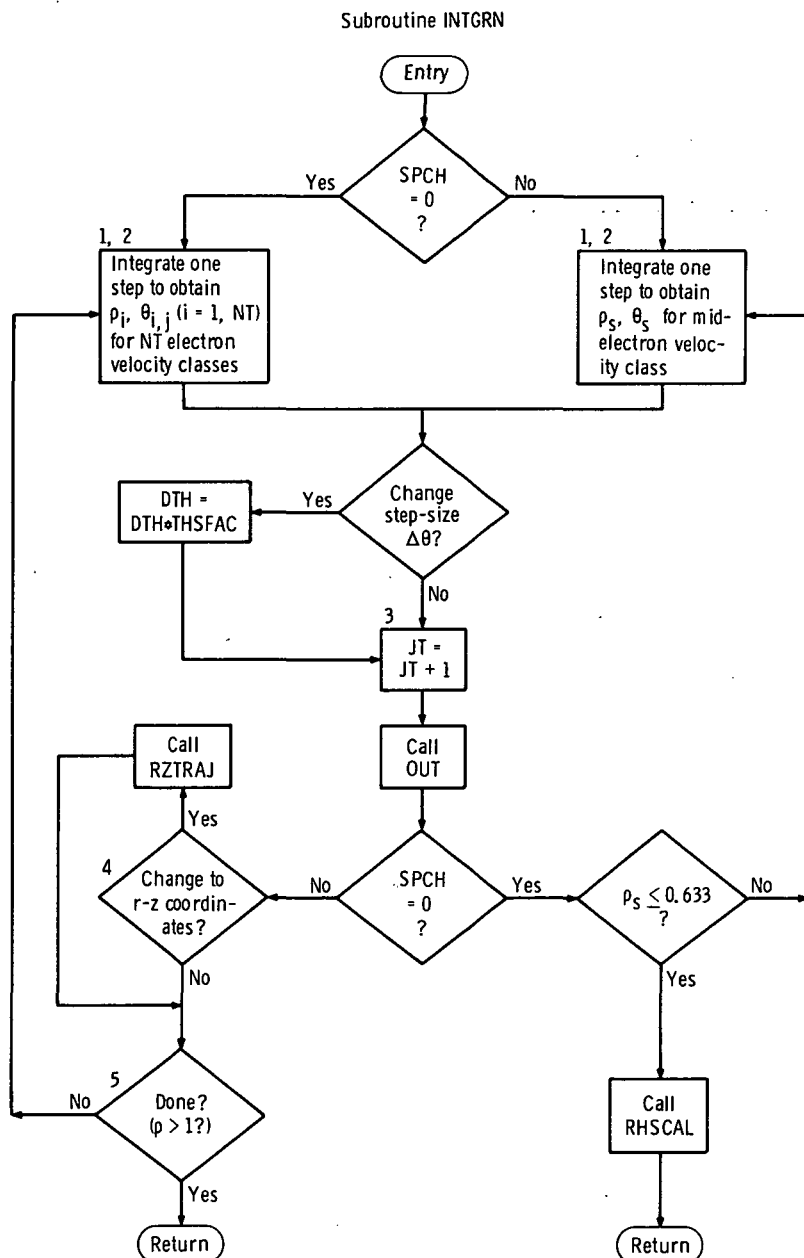
RHM(17)	ρ -mesh values
RHOP(10)	ρ'
RHOPP(10)	ρ''
RHRZ	ρ in r-z coordinate system
RHT(10)	ρ -values for each trajectory
RHV(10)	ρ -values for equipotential lines
SPCH	space charge indicator switch
ST, ST2	$\sin \theta, \sin^2 \theta$
T0, T1, T2, . . .	temporary storages
TA(25)	θ -mesh values
TAU02	τ_0^2
TH	variable of integration, θ
TH0	initial cone angle, deg
TH1	initial cone angle, deg
TH2	collector angle at which surface charge is zero, deg
THD(10)	$\dot{\theta}$ array
THF	θ_f
THMD(25)	θ -mesh values, deg
THSDEL	θ step-size increment, deg
THSW	θ switch for step-size control
THTD(10)	θ -coordinate of trajectory, deg
THD2	$\dot{\theta}^2$
THTR	θ -coordinate of trajectory, rad
THRZ	θ in r-z coordinate system
V(17, 25)	potential inside spherical collector
V0	initial normalized electrical potential, V_0
VR	interpolated potential in r-z system
VSMI(10)	v_i array; beam velocities
VT(10)	array of initial voltages
W(16)	Runge-Kutta storage area in r-z system

XCTR	value of source term at center of sphere
XT(25, 16)	source term needed for solution to Poisson's equation
Y(16)	Runge-Kutta storage area in ρ - θ system
Z, ZP	$z, z'(\partial z / \partial r)$
Z1P	z'_1
Z2, Z2P	z'_2, z'_2
	miscellaneous storages for independent variables in cylindrical coordinate system
ZJ0	initial current density, J_0 , A/cm ²
ZI0	initial current, I_0 , A
ZKP	perveance, K_p , A/V ^{3/2}
ZED	rectilinear coordinate, z

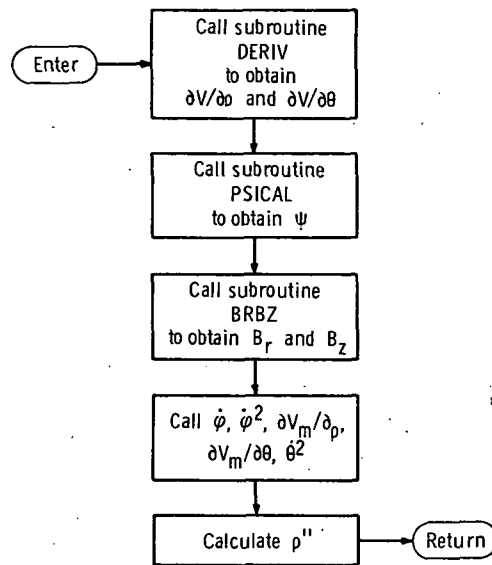
APPENDIX D

FLOW CHARTS

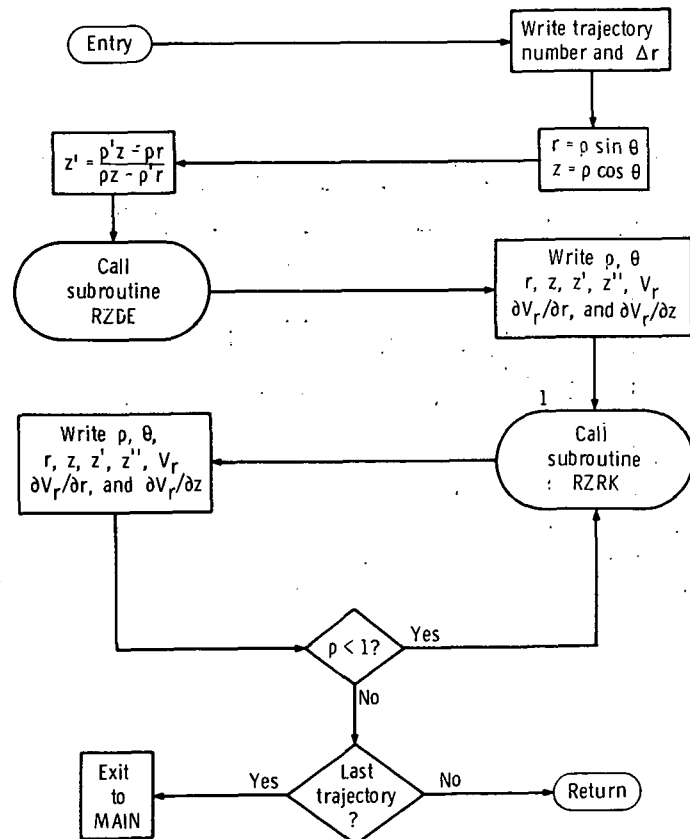
Flow charts are presented only for those five subroutines, INTGRN, DE, RZTRAJ, VFIELD, RHSCAL, which might not otherwise be easily understood. Diamond-shaped blocks indicate decision-making points in the subroutines. Numbers appearing on blocks refer to the corresponding FORTRAN statement numbers in the subroutines.



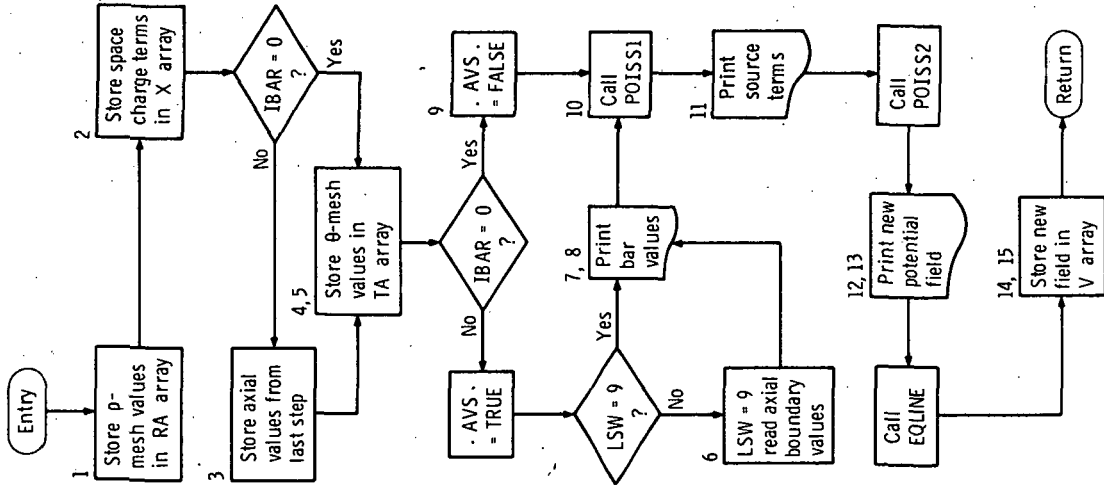
Subroutine DE



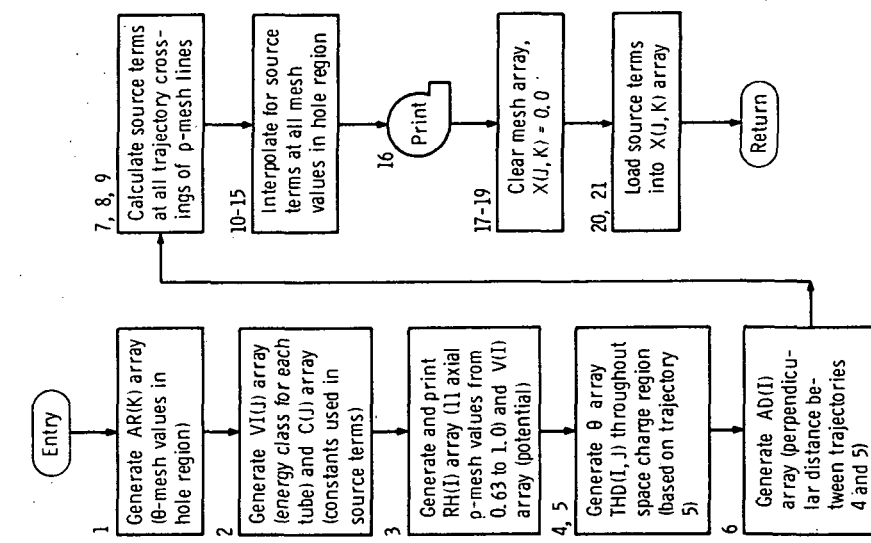
Subroutine RZTRAJ



Subroutine VFIELD



Subroutine RHSCAL



APPENDIX E

MAGNETIC FIELD CALCULATIONS

$$B_z^0(0, z) = \frac{B_0}{\pi} \left[\pi - \tan^{-1} \left(\frac{a}{z} \right) - \frac{x}{1+x^2} \right] \quad (E1)$$

where $x = z/a$. Then,

$$\begin{aligned} B_z^I(0, z) &= - \frac{2B_0}{\pi a} \times \frac{1}{(1+x^2)^2} \\ B_z^{II}(0, z) &= \frac{8B_0 x}{\pi a^2} \times \frac{1}{(1+x^2)^3} \\ B_z^{III}(0, z) &= \frac{8B_0}{\pi a^3} \times \frac{1 - 5x^2}{(1+x^2)^4} \\ B_z^{IV}(0, z) &= - \frac{48B_0 x}{\pi a^4} \times \frac{3 - 5x^2}{(1+x^2)^5} \\ B_z^V(0, z) &= - \frac{48B_0}{\pi a^5} \times \frac{3 - 42x^2 + 35x^4}{(1+x^2)^6} \\ B_z^{VI}(0, z) &= \frac{4 \times 480B_0 x}{\pi a^6 (1+x^2)^7} (3 - 14x^2 + 7x^4) \\ B_z^{VII}(0, z) &= \frac{12 \times 480B_0}{\pi a^7 (1+x^2)^8} (1 - 27x^2 + 63x^4 - 21x^6) \\ B_z^{VIII}(0, z) &= - \frac{12 \times 14 \times 480B_0 x}{\pi a^8 (1+x^2)^9} (5 - 45x^2 + 63x^4 - 15x^6) \\ B_z^{IX}(0, z) &= - \frac{12 \times 14 \times 480B_0}{\pi a^9 (1+x^2)^{10}} (5 - 220x^2 + 990x^4 - 924x^6 + 165x^8) \\ B_z^{X}(0, z) &= \frac{14 \times 48 \times 480B_0 x}{\pi a^{10} (1+x^2)^{11}} (135 - 1980x^2 + 5346x^4 - 3564x^6 + 495x^8) \\ B_z^{XI}(0, z) &= \frac{14 \times 45 \times 48 \times 480B_0}{\pi a^{11} (1+x^2)^{12}} (3 - 195x^2 + 1430x^4 - 2574x^6 + 1287x^8 - 143x^{10}) \\ B_z^{XII}(0, z) &= - \frac{28 \times 45 \times 48 \times 480B_0 x}{\pi a^{12} (1+x^2)^{13}} (231 - 5005x^2 + 22022x^4 - 28314x^6 + 11011x^8 - 1001x^{10}) \end{aligned} \quad (E2)$$

To simplify these expressions, let

$$\left. \begin{aligned}
 T_3 &= 1 - 5x^2 \\
 T_4 &= 3 - 5x^2 \\
 T_5 &= 3 - 42x^2 + 35x^4 = 3 - 7x^2(6 - 5x^2) \\
 T_6 &= 3 - 14x^2 + 7x^4 = 3 - 7x^2(2 - x^2) \\
 T_7 &= 1 - 27x^2 + 63x^4 - 21x^6 = 1 - 3x^2[9 - 7x^2(3 - x^2)] \\
 T_8 &= 5 - 45x^2 + 63x^4 - 15x^6 = 5 - 3x^2[15 - x^2(21 - 5x^2)] \\
 T_9 &= 5 - 220x^2 + 990x^4 - 924x^6 + 165x^8 = 5 - 11x^2[20 - 3x^2[30 - x^2(28 - 5x^2)]] \\
 T_{10} &= 135 - 1980x^2 + 5346x^4 - 3564x^6 + 495x^8 \\
 &\quad = 9(15 - 11x^2[20 - x^2[54 - x^2(36 - 5x^2)]]) \\
 T_{11} &= 3 - 195x^2 + 1430x^4 - 2574x^6 + 1287x^8 - 143x^{10} \\
 &\quad = 3 - 13x^2(15 - 11x^2[10 - x^2[18 - x^2(9 - x^2)]]) \\
 T_{12} &= 231 - 5005x^2 + 22022x^4 - 28314x^6 + 11011x^8 - 1001x^{10} \\
 &\quad = 11[21 - 13x^2(35 - x^2[154 - x^2[198 - 7x^2(11 - x^2)]])]
 \end{aligned} \right\} \quad (E3)$$

Then, substituting these expressions for those in (E2), we now have

$$\left. \begin{aligned}
B_z^I(0, z) &= - \frac{2B_0}{\pi a^2 (1+x^2)^2} \\
B_z^{II}(0, z) &= \frac{8B_0 x}{\pi a^2 (1+x^2)^3} \\
B_z^{III}(0, z) &= \frac{8B_0 T_3}{\pi a^3 (1+x^2)^4} \\
B_z^{IV}(0, z) &= - \frac{48B_0 x T_4}{\pi a^4 (1+x^2)^5} \\
B_z^{V}(0, z) &= - \frac{48B_0 T_5}{\pi a^5 (1+x^2)^6} \\
B_z^{VI}(0, z) &= \frac{4 \times 480 B_0 x T_6}{\pi a^6 (1+x^2)^7} \\
B_z^{VII}(0, z) &= \frac{12 \times 480 B_0 T_7}{\pi a^7 (1+x^2)^8} \\
B_z^{VIII}(0, z) &= - \frac{12 \times 14 \times 480 B_0 x T_8}{\pi a^8 (1+x^2)^9} \\
B_z^{IX}(0, z) &= - \frac{12 \times 14 \times 480 B_0 T_9}{\pi a^9 (1+x^2)^{10}} \\
B_z^{X}(0, z) &= \frac{14 \times 48 \times 480 B_0 x T_{10}}{\pi a^{10} (1+x^2)^{11}} \\
B_z^{XI}(0, z) &= \frac{14 \times 45 \times 48 \times 480 B_0 T_{11}}{\pi a^{11} (1+x^2)^{12}} \\
B_z^{XII}(0, z) &= - \frac{28 \times 45 \times 48 \times 480 B_0 x T_{12}}{\pi a^{12} (1+x^2)^{13}}
\end{aligned} \right\} \quad (E4)$$

Since

$$B_r(r, z) = -B^I(0, z) \frac{r}{2} + \frac{1}{1! 2!} B^{III}(0, z) \left(\frac{r}{2}\right)^3 - \frac{1}{2! 3!} B^V(0, z) \left(\frac{r}{2}\right)^5 + \frac{1}{3! 4!} B^{VII}(0, z) \left(\frac{r}{2}\right)^7 - \dots \quad (E5)$$

We make the substitution $r_2 = r/2$, and nest as follows,

$$B_r(r, z) = -r_2^2 \left[B^I - \frac{r_2^2}{1 \times 2} \left(B^{III} - \frac{r_2^2}{2 \times 3} \left\{ B^V - \frac{r_2^2}{3 \times 4} \left[B^{VII} - \frac{r_2^2}{4 \times 5} \left(B^I - \frac{B^{XI} r_2^2}{5 \times 6} - \dots \right) \right] \right\} \right) \right] \quad (E6)$$

and similarly,

$$B_z(r, z) = B^0 - r_2^2 \left[B^{II} - \frac{r_2^2}{2^2} \left(B^{IV} - \frac{r_2^2}{3^2} \left\{ B^{VI} - \frac{r_2^2}{4^2} \left[B^{VIII} - \frac{r_2^2}{5^2} \left(B^{X} - \frac{r_2^2}{6^2} B^{XII} - \dots \right) \right] \right\} \right) \right] \quad (E7)$$

APPENDIX F

DERIVATION OF EQUATIONS OF MOTION

The equations of motion as derived in reference 1, equations (B17) and (B18), are

$$\rho' \ddot{\theta} = \rho \dot{\theta}^2 + \rho \sin^2 \theta \dot{\phi}^2 - \rho'' \dot{\theta}^2 + \frac{\eta}{R^2} \frac{\partial V}{\partial \rho} - \frac{\eta}{R} \sin \theta \dot{\phi} A_\varphi - \frac{\eta}{R} \rho \sin \theta \dot{\phi} \frac{\partial A_\varphi}{\partial \rho} \quad (F1)$$

$$\ddot{\theta} = -\frac{2\rho' \dot{\theta}^2}{\rho} + \sin \theta \cos \theta \dot{\phi}^2 + \frac{\eta}{\rho^2 R^2} \frac{\partial V}{\partial \theta} - \frac{\eta}{\rho R} \cos \theta \dot{\phi} A_\varphi - \frac{\eta}{\rho R} \sin \theta \dot{\phi} \frac{\partial A_\varphi}{\partial \theta} \quad (F2)$$

Solving these two equations simultaneously for ρ'' yields

$$\rho'' = \rho + \frac{\rho \sin^2 \theta \dot{\phi}^2}{\dot{\theta}^2} + \frac{\eta}{R \dot{\theta}^2} f_1 + \frac{2\rho'^2}{\rho} - \frac{\rho' \sin \theta \cos \theta \dot{\phi}^2}{\dot{\theta}^2} - \frac{\rho' \eta}{\rho^2 R^2 \dot{\theta}^2} f_2 \quad (F3)$$

where

$$\left. \begin{aligned} f_1 &= \frac{1}{R} \frac{\partial V}{\partial \rho} - \sin \theta A_\varphi \dot{\phi} - \rho \sin \theta \dot{\phi} \frac{\partial A_\varphi}{\partial \rho} \\ f_2 &= \frac{\partial V}{\partial \theta} - \rho R \cos \theta A_\varphi \dot{\phi} - \rho R \sin \theta \dot{\phi} \frac{\partial A_\varphi}{\partial \theta} \end{aligned} \right\} \quad (F4a)$$

or, using the relations described in appendix D of reference 1, these expressions may be rewritten

$$\left. \begin{aligned} f_1 &= \frac{1}{R} \frac{\partial V}{\partial \rho} - \sin \theta \dot{\phi} \frac{\partial V_m}{\partial \theta} \\ f_2 &= \frac{\partial V}{\partial \theta} + \rho^2 R \sin \theta \dot{\phi} \frac{\partial V_m}{\partial \rho} \end{aligned} \right\} \quad (F4b)$$

Away from the entry hole, the magnetic field terms $\dot{\phi}$, A_φ , and V_m are negligible. Therefore, in this region equation (F3) may be expressed

$$\rho'' = \rho + \frac{\eta}{R^2 \dot{\theta}^2} \times \frac{\partial V}{\partial \rho} + \frac{2\rho'^2}{\rho} - \frac{\rho' \eta}{\rho^2 R^2 \dot{\theta}^2} \times \frac{\partial V}{\partial \theta} \quad (F5)$$

using equation (B16) of reference 1 as

$$\dot{\theta}^2 = \frac{2\eta V_0 (\epsilon_i + V)}{R^2 \rho^2 \left[1 + \left(\frac{\rho'}{\rho} \right)^2 \right]} \quad (F6)$$

and, with the appropriate substitutions, we may express this equation in cylindrical coordinates

$$z'' = \frac{\frac{\partial V}{\partial z} - z' \frac{\partial V}{\partial r}}{2 \left[\frac{\epsilon_i + V}{1 + (z')^2} \right]}$$

APPENDIX G

MATHEMATICAL SYMBOLS

A	area of annulus, cm^2
a	radius of collector entry hole, cm
B_r	r -component of potential field, $\partial V_m / \partial r$, G/cm
B_z	z -component of potential field, $\partial V_m / \partial z$, G/cm
B_0	magnetic flux density, G
b	radius of electron beam at injection, cm
E	$v_i + V$
I	current, A
J	current density, A/cm^2
K_p	perveance, $\text{A}/V^{3/2}$
R	unreduced radius of spherical collector, cm
r, z	cylindrical coordinates
u	electron energy
V	normalized electric potential
V_m	magnetic field potential
V_r	$\partial V / \partial r$
V_z	$\partial V / \partial z$
V_ρ	$\partial V / \partial \rho$
V_θ	$\partial V / \partial \theta$
v_i	i^{th} normalized injection energy class
ϵ_0	permittivity of free space, $8.86 \times 10^{-14} \text{ F/cm}$
η_e	electron charge-mass ratio, charge/kg $\times 10^{11}$
ρ	normalized radius vector
$\bar{\rho}$	unnormalized radius vector, cm
ρ_e	space charge density, C/cm^3
τ_0	$R/(2\eta V_0)^{1/2}$
θ, φ	polar and azimuthal spherical coordinate angles

REFERENCES

1. Kosmahl, Henry G.: A Novel, Axisymmetric, Electrostatic Collector for Linear Beam Microwave Tubes. NASA TN D-6093, 1971.
2. Reese, Oliver W.: Numerical Method and FORTRAN Program for Solving Poisson's Equation Over Axisymmetric Regions of a Sphere. NASA TN D-6438, 1971.



NASA 451

POSTMASTER: If Undeliverable (Section 158
Postal Manual) Do Not Return

"The aeronautical and space activities of the United States shall be conducted so as to contribute . . . to the expansion of human knowledge of phenomena in the atmosphere and space. The Administration shall provide for the widest practicable and appropriate dissemination of information concerning its activities and the results thereof."

— NATIONAL AERONAUTICS AND SPACE ACT OF 1958

NASA SCIENTIFIC AND TECHNICAL PUBLICATIONS

TECHNICAL REPORTS: Scientific and technical information considered important, complete, and a lasting contribution to existing knowledge.

TECHNICAL NOTES: Information less broad in scope but nevertheless of importance as a contribution to existing knowledge.

TECHNICAL MEMORANDUMS: Information receiving limited distribution because of preliminary data, security classification, or other reasons.

CONTRACTOR REPORTS: Scientific and technical information generated under a NASA contract or grant and considered an important contribution to existing knowledge.

TECHNICAL TRANSLATIONS: Information published in a foreign language considered to merit NASA distribution in English.

SPECIAL PUBLICATIONS: Information derived from or of value to NASA activities. Publications include conference proceedings, monographs, data compilations, handbooks, sourcebooks, and special bibliographies.

TECHNOLOGY UTILIZATION PUBLICATIONS: Information on technology used by NASA that may be of particular interest in commercial and other non-aerospace applications. Publications include Tech Briefs, Technology Utilization Reports and Technology Surveys.

Details on the availability of these publications may be obtained from:

SCIENTIFIC AND TECHNICAL INFORMATION OFFICE

NATIONAL AERONAUTICS AND SPACE ADMINISTRATION

Washington, D.C. 20546